IEEE Access
Multidisciplinary | Rapid Review | Open Access Journal

Received September 13, 2020, accepted September 24, 2020, date of publication September 28, 2020,
date of current version October 8, 2020.

Digital Object Identifier 10.1109/ACCESS.2020.3027436

Performance Analysis of APSO and Firefly Algorithm for Short Term Optimal Scheduling of Multi-Generation Hybrid Energy System

SHEROZE LIAQUAT[1], MUHAMMAD SALMAN FAKHAR[2], SYED ABDUL RAHMAN KASHIF[2], AKHTAR RASOOL[3], OMER SALEEM[1], (Member, IEEE), AND SANJEEVIKUMAR PADMANABAN[4], (Senior Member, IEEE)

[1]Department of Electrical Engineering, National University of Computer and Emerging Sciences, Lahore 54000, Pakistan
[2]Department of Electrical Engineering, University of Engineering and Technology, Lahore 54000, Pakistan
[3]Department of Electrical Engineering, Sharif College of Engineering and Technology, Lahore 34956, Pakistan
[4]Department of Energy Technology, Aalborg University, 6700 Esbjerg, Denmark

Corresponding author: Sheroze Liaquat (shahroze.liaquat@nu.edu.pk)

ABSTRACT This paper presents a modified and novel form of the conventional short-term hydrothermal scheduling problem by incorporating the effects of adding the photovoltaic energy source to the conventional grid. A photovoltaic energy source is intermittent in nature, therefore, to determine the optimal power contribution of the photovoltaic source towards the economic dispatch problem, a detailed strategy is presented in this paper. The proposed design method includes the forecasting of the photovoltaic system's parameters using the Auto-Regressive Integrated Moving Average (ARIMA) model. The analytical model is developed based on the fractional integral polynomials for studying the characteristics of the single photovoltaic module. The optimization of power allocation in the system consisting of conventional and non-conventional energy sources is highly non-linear and classical deterministic methods can not be guaranteed to determine the optimal solution for economic power dispatch. The global optima of such non-linear and non-convex problems can be determined using swarm-based intelligence techniques. This paper presents accelerated particle swarm optimization and the firefly algorithm to determine a solution for short-term non-linear scheduling problems. The multiple test cases have been presented to demonstrate the effectiveness of the proposed solution over classical methods. The overall generation cost of the selected hybrid system is reduced using the proposed methods while meeting the generation constraints of each energy source. Moreover, due to the stochastic nature of the meta-heuristic techniques, a comprehensive statistical comparison, based on the independent T-test results, is also presented to highlight the algorithm which performs better for selected scheduling problems. It has been demonstrated that accelerated particle swarm optimization gives lower mean generation cost of the system whereas the execution time of the firefly algorithm is better compared to its counterpart.

INDEX TERMS Mathematical modeling, auto-regressive integrated moving average model, accelerated particle swarm optimization, firefly algorithm, short term hydrothermal scheduling, independent t-test.

I. INTRODUCTION

A. PROBLEM STATEMENT

The renewable energy systems are now being extensively used in addition to the conventional sources in order to meet the load demand over the entire scheduling period due to their sustainable and environmental friendly nature [1]–[3]. The problem of the coordination between the different types of energy resources is a major task for planning engineers and the research is still in progress for optimal utilization of all these resources such that the sum of the power contribution from all these resources equals the load demand over the particular scheduling interval while meeting the certain generation constraints of each energy source [4]–[6]. The problem of the coordination of these energy resources also known as the Economic Dispatch (ED) problem in the context is of the

The associate editor coordinating the review of this manuscript and approving it for publication was Jagdish Chand Bansal.

special interest in the field of optimization theory. A number of deterministic as well as the swarm based intelligence techniques are being explored by the researchers over the past few years to find the optimal solution of this particular optimization problem [7], [8]. The two major conventional energy resources being used are the thermal energy source and the hydroelectric source each having its own possible generation constraints. The economic dispatch problem including these two conventional sources is known as the Short Term Hydrothermal Scheduling (STHTS) problem in literature.

B. LITERATURE REVIEW

There are number of techniques discussed in the literature which find the optimal solution of the aforementioned problem. The work in [9] solves the short term hydrothermal scheduling problem while using the genetic algorithm and involves the future and immediate cost functions for the comparison purposes. The genetic algorithm (GA) proposed in this research outperforms the techniques like dynamic programming and lagrangian relaxation method for a test case which consists of ten thermal and eleven hydroelectric sources. The work in [10] solves the hydrothermal scheduling problem using the fuzzy technique by considering the multi-objective function which includes both the fuel and the emission cost of the thermal generation. The work in [11] suggests the cascaded connection of the reservoirs in the hydrothermal scheduling problem and the valve point effect for the thermal generation and solves the proposed problem using the Particle Swarm Optimization (PSO) algorithm. The work in [12] addresses the same problem while considering the valve point effect for the thermal generation. In [12], the author uses the Teaching Learning based Optimization (TLBO) technique and compares its performance with the techniques like APSO, Evolutionary technique (ET) and Hybrid Differential Evolution (HDE) method. The suggested technique outperforms the remaining methods in the terms of the convergence of the algorithm towards the minimum generation cost. The work in [13] uses the evolutionary programming techniques while considering the valve point effect and the prohibited operating zones constraint. The author suggests the Gaussian and Cauchy mutation based evolutionary programming methods to solve the multiple test cases and compares the performance of these different techniques. The work in [14] uses the Cuckoo Search Algorithm (CSA) to solve the hydrothermal scheduling problem while considering the valve point effect and the transmission losses of the system. The author compares the performance of the CSA with the genetic algorithm and concludes that CSA outperforms the genetic algorithms. The work in [15] uses the hybrid abc-bat algorithm for finding the optimal solution of the proposed scheduling problem and compares its performance with the other hybrid techniques like hybrid PSO. Similarly, s [16]–[18] discuss the hydrothermal scheduling problem using different techniques while considering the multiple generation constraints.

All the above mentioned work contributes effectively towards solution of the conventional short term hydrothermal scheduling problem by using the different algorithms but with the increasing number of the distributed generation systems being integrated to the grid, the problem of adjusting these renewable energy sources with the conventional ones is of the special interest and the research is still in progress to develop the certain scenarios in order to compensate the inclusion of these renewable energy resources to the existing systems. The thermal solar economic dispatch has been discussed in the literature using the different optimization techniques. The work in [19] considers the system which consists of multiple solar units integrated with the thermal generation and uses the mixed integer programming to solve the proposed problem. The two cases are explored by the authors, the first attempts to increase the solar share towards the dispatch problem while the second decreases the cost of the solar power generation. The work in [20] considers the wind and photovoltaic sources in addition to the conventional sources and uses the mixed integer programming technique to solve the problem. The forecasted wind and solar power curves are used for the dispatch problem while considering the two cases. The first case excludes the hydro energy source while finding the optimal dispatch of the thermal and renewable energy sources to meet the load demand. The second case includes the hydro and pumped energy storage in addition to the renewable and thermal sources. The work in [21] uses the robust optimization technique to solve the dispatch problem and uses the hybrid energy system which consists of the conventional (thermal and hydro) and non conventional sources (wind and solar) as the test case. It minimizes the total generation cost while considering the intermittent nature of the renewable sources. The work in [22] uses the firefly algorithm and solves the economic dispatch problem while considering the wind and solar sources. The authors formulate an objective function which includes the solar, wind and thermal generation cost while considering the penalty costs for compensating the uncertainty of the power output of the non conventional sources. The work in [23] uses the firefly algorithm and solves the economic dispatch problem while considering the wind and solar sources. The authors formulate an objective function which includes the solar, wind and thermal generation cost while considering the penalty costs for compensating the uncertainty of the power output of the non conventional sources. Similarly, [24]–[26] find the combined economic dispatch of the conventional and non-conventional energy resources.

C. RESEARCH GAP AND CONTRIBUTIONS

The mentioned references consider the renewable energy resources mostly with the thermal generation alone. The STHTS problem has not been discussed extensively with the renewable sources. Moreover, majority of the work uses the forecasted wind and solar power for different scheduling intervals without using the real time data and providing the sufficient mathematical details. In majority of the mentioned references, the comparison between the two algorithms for a particular problem is carried out without providing any

statistical analysis. In order to overcome this research gap, the **major contributions** of this research are as follows:

1) Propose a modified form of the short term hydrothermal scheduling problem by adding the PV energy source to the grid.
2) To make the problem more practical, use the real time data for the input parameters of the PV system and forecast the day ahead irradiance and temperature levels using ARIMA model.
3) Suggest a comprehensive PV system design to predict the solar power share using the forecasted parameters and developed mathematical model for PV module.
4) Implement the APSO and Firefly techniques for the suggested problem for multiple test cases while considering the various generation constraints.
5) Use the independent t-test results to statistically compare the performance of the two algorithms

The remaining paper is organized as follows. The Section 2 describes the overview of algorithms and the proposed system configuration. The Section 3 describes the photovoltaic system design. The Section 4 describes the methodology and the results for various test cases. The Section 5 presents the statistical comparison of algorithms. The Section 6 concludes the findings of the proposed research.

II. OVERVIEW OF META-HEURISTIC ALGORITHMS AND PROPOSED MODEL

The application of the meta-heuristic algorithms in determining the optimal solution of the various complex optimization problems is increasing due to their stochastic and deterministic ability. Moreover, they also help to find good approximate to global solution of such complex optimization problems. In most applications, the objective function is highly nonlinear, multi-modal or complex in nature and it becomes difficult to find the global optimum of such functions using the classical deterministic techniques like Newton Method, Gradient method or Lagrange multiplier method. The swarm based intelligence techniques are useful in such circumstances and provide a solution of such complex problems which is quite near to the global optimum and reduce the computational effort by a significant factor. A number of such algorithms have been described in the literature and the research is still in progress in order to improve their performance. The suggested techniques, the APSO and the Firefly algorithm are easier to implement and give promising results in the terms of finding the global optimum of various complex optimization problems [27]–[29].

A. FIREFLY ALGORITHM

The firefly algorithm is based on the behavior of the fireflies in nature. The brightness of the fireflies is the major phenomenon which dictates the working of this algorithm and its convergence towards the optimal solution. The fireflies form the possible solution set of the given optimization problem and the dimensions of each firefly are dictated by the number of the decision variables of the objective function. The light intensity or the brightness of the fireflies depends upon the distance between the two fireflies [30]–[32] and is given by the inverse square law as follows:

$$F(r) = \frac{F_s}{r^2} \tag{1}$$

where, F_r is the light intensity at distance r from source and F_s represents the source intensity. If the light absorption coefficient of the medium is defined by γ_{abs}, then we can define the intensity of the fireflies by (2).

$$F = F_o e^{-\gamma_{abs} r} \tag{2}$$

In order to avoid the singularity for $r = 0$ in (1), we can combine the above two equations to define the light intensity F in the terms of the distance r and absorption coefficient γ_{abs} as follows:

$$F(r) = F_o e^{-\gamma_{abs} r^2} \tag{3}$$

where, F_o is the light intensity for $r = 0$. We can define the attractiveness of the fireflies β by the following two relations:

$$\beta = \beta_o e^{-\gamma_{abs} r^2} \tag{4}$$

$$\beta = \frac{\beta_o}{1 + \gamma_{abs} r^2} \tag{5}$$

We can represent the characteristic distance by ζ which defines the attractiveness value to be equal to β_o/e for (4) or $\beta_o/2$ for (5). In most cases, the attractiveness is taken to be the decreasing function defined by (7).

$$\zeta = \frac{1}{\sqrt{\gamma_{abs}}} \tag{6}$$

$$\beta = \beta_o e^{-\gamma_{abs} r^n} \quad (n \geq 1) \tag{7}$$

In order to compute the distance between the two fireflies m and n, the distance relation is given in (8). For a two dimensional space having coordinates A and B, the distance relation is given in (9).

$$D_{mn} = ||X_m - X_n|| = \sqrt{\sum_{i=1}^{D} (X_{m,i} - X_{n,i})^2} \tag{8}$$

$$D_{mn} = ((A_m - A_n)^2 + (B_m - B_n)^2)^{\frac{1}{2}} \tag{9}$$

where, $X_{m,i}$ represents the *ith* component of the X_m coordinate of the firefly m. The movement of the firefly m towards the brighter firefly n is given by the update relation in (10).

$$X_m = X_m + \beta_o e^{-\gamma_{abs} r_{mn}^2} (X_n - X_m) + \alpha(rand - 0.5) \tag{10}$$

where, α is in the range [0,1] and rand represents the random numbers generated in the range [0,1]. In most of the cases we can take the value of β_o to be equal to 1. The value of γ_{abs} for most of the optimization problems is usually given in the range [0.1,10]. The selection of the absorption coefficient γ_{abs} is extremely important for the performance of the firefly algorithm and the convergence of the algorithm

towards the optimal solution depends upon its proper tuning. For example, if we take the value of γ_{abs} to be equal to zero then we have $\beta = \beta_o$. In other words the light intensity or the attractiveness remains constant and does not decrease in the medium and is independent of the medium's absorption coefficient γ_{abs}. On the other hand if we take $\gamma_{abs} \to \infty$, then the process becomes a random process. Therefore, we have to optimally select the value of γ_{abs} with in these two extremes to optimize the behavior of the algorithm for the given optimization problem [33].

B. ACCELERATED PARTICLE SWARM OPTIMIZATION

Particle Swarm Optimization (PSO) is another powerful swarm based algorithm which has extensively been used by many researchers to find the optimal solution of the different optimization problems. The possible solutions of the given objective function known as the particles in this case are generated randomly and the position of these particles is updated using the certain update rules. The dimensions of the particles again depend upon the number of the decision variables involved in the concerned objective function. This algorithm is based upon the behavior of the swarm and uses the similar concept to reach towards the optimal solution of the given optimization problem. The two major components which influence the movement of the particles towards the optimal solution are the particle's own best position X_i' and the global best position g' among all the particles [11], [34]. The velocity component V_i and the position component X_i of the i particle are updated using the following relations:

$$V_i^{t+1} = V_i^t + \alpha_1 c_1 \odot (g' - X_i^t) + \alpha_2 c_2 \odot (X_i' - X_i^t) \quad (11)$$

$$X_i^{t+1} = X_i^t + V_i^{t+1} \quad (12)$$

where, constants c_1 and c_2 are randomly generated in the range [0,1]. The constants α_1 and α_2 are known as the acceleration constants. The sum of these constants is given as $\sum_{i=1}^{2} \alpha_i = 4$ where both the constants are assumed to be equal to 2. In (11), we can introduce the inertia constant ω to further improve the movement of the particles and hence the update equation for the velocity component after introducing the inertia constant is given as:

$$V_i^{t+1} = \omega V_i^t + \alpha_1 c_1 \odot (g' - X_i^t) + \alpha_2 c_2 \odot (X_i' - X_i^t) \quad (13)$$

where the inertia weight ω is given in the range of 0 to 1. The typical value of ω for most cases is usually from 0.5 to 0.9. Accelerated Particle Swarm Optimization is a well known variant of the conventional PSO algorithm which uses only the global best position g' to further improve the convergence behavior of the algorithm. Therefore, the velocity component and the position component in the case of the APSO are given as follows:

$$V_i^{t+1} = V_i^t + \alpha_1 (c_1 - 0.5) + \alpha_2 (g' - X_i) \quad (14)$$

$$X_i^{t+1} = X_i^t + V_i^{t+1} \quad (15)$$

The single update equation for APSO can be written by (16) to further improve the performance of algorithm.

$$X_i^{t+1} = (1 - \alpha_2) X_i^t + \alpha_2 g' + \alpha_1 (c_1 - 0.5) \quad (16)$$

In the case of APSO, the values of α_1 and α_2 are usually 0.2 and 0.5 respectively. The random part of the APSO can be taken as the decreasing function to further improve the algorithm's performance. The decreasing function for the randomness can be written as follow:

$$\alpha_1 = \alpha_0 \beta^t \quad (17)$$

The range of β is given as (0,1) and the initial value for α_0 can be taken with in the range [0.5,1]. The steps of the APSO and Firefly algorithm will be further elaborated using the proposed problem in the later sections.

C. SYSTEM CONFIGURATION

The proposed system configuration consists of one hydroelectric energy source, one equivalent thermal generation and one equivalent solar energy source of the given rated capacity. Fig 1 shows the equivalent model of the proposed system. The main objective of the hydrothermal scheduling problem is to minimize the fuel cost of the thermal plant without violating the system constraints. The concerned dispatch problem consists of nine different scheduling intervals each of equal duration (one hour). The load is considered to be dynamic in nature with each scheduling interval having different load demand. The next section covers the detailed analysis of the PV design which is the first step in solving the suggested dispatch problem.

III. PHOTOVOLTAIC SYSTEM DESIGN

The first step to find the economic dispatch of the suggested hybrid energy system is to find the power contribution of the PV source for different scheduling intervals. The output power of the PV source is fluctuating in nature and depends upon the external atmospheric parameters (irradiance and temperature levels). In order to accurately predict the PV source power share towards the dispatch problem, following design steps as shown in Fig. 1 are suggested:

1) Develop the mathematical model for single PV module to show the effect of major input parameters of PV system on the IV characteristics and the power curves of the module.
2) Forecast the major atmospheric parameters using the ARIMA model. The forecasted parameters will be used as an input for the mathematical model developed for the PV system to determine the optimal solar power.
3) Find the solar power for different scheduling intervals using the developed mathematical model and the forecasted parameters.

A. MATHEMATICAL MODELING OF PV MODULE

A number of the mathematical models have been discussed in the literature which model the behavior of the photovoltaic

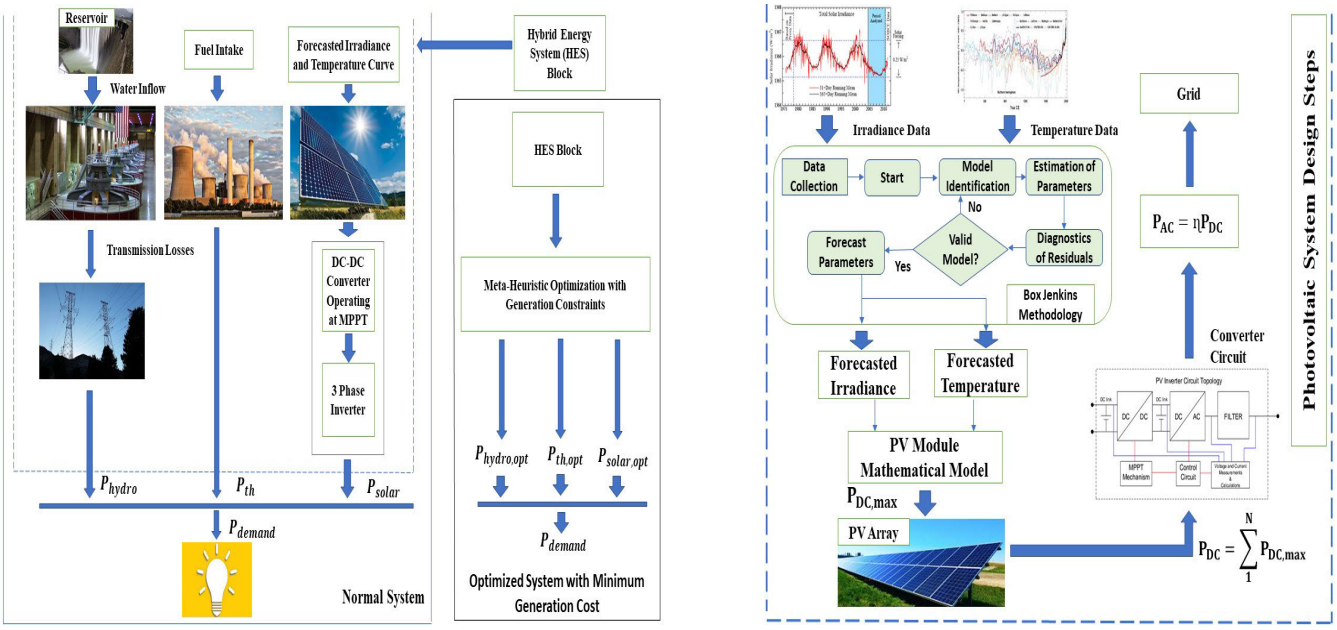

FIGURE 1. Flow chart for different energy systems. (a) Suggested hybrid energy system. (b) Photovoltaic system design.

module and its dependence on the atmospheric conditions [35], [36]. The mathematical model is developed in accordance with [37] to find the power contribution of the PV system by modeling the characteristics of a single PV module. The two major parameters for determining the characteristics of the PV module are the Irradiance and the Temperature levels. The proposed model takes into account these variable parameters and determines the I-V characteristics and the power curves of the PV module under the changing atmospheric conditions. The relation given by (18) determines the current of the PV module as the voltage function given as follows:

$$I(U) = I'_{sc} - I'_{sc}\,(\frac{U}{U'_{oc}})^{\alpha+\beta} \tag{18}$$

where, I'_{sc} represents the PV module short circuit current at arbitrary irradiance and temperature level. U'_{oc} represents the PV module open circuit voltage at arbitrary irradiance and temperature level. U is the output voltage of the module given in the range $0 \leq \mathrm{U} \leq U'_{oc}$. I represents the output current of the module given in the range $0 \leq \mathrm{I} \leq I'_{sc}$. $\alpha + \beta$ represnts the sum of a non-negative integer α and an integer β in the range $0 \leq \beta < 1$. The power of the photovoltaic module is determined by the product of the output voltage U and the current of the module as the function of the voltage $I(U)$ and is given in (19).

$$P(U) = I(U).U = (I'_{sc} - I'_{sc}\,(\frac{U}{U'_{oc}})^{\alpha+\beta})\,U \tag{19}$$

Equation 18 shows the dependence of the current I on the three major parameters, U'_{oc}, I'_{sc} and $\alpha + \beta$ sum. In order to determine these parameters the relations (20)-(22) are used.

$$U'_{oc} = s_i.\frac{E}{E_{STC}}.TCV.(T - T_{STC}) + U_{max} - (U_{max} - U_{min}).exp(\frac{E}{E_{STC}}.ln(\frac{U_{max} - U_{oc}}{U_{max} - U_{min}})) \tag{20}$$

$$I'_{sc} = p_i.\frac{E}{E_{STC}}.(I_{sc} + TCI.(T - T_{STC})) \tag{21}$$

$$\alpha + \beta = \frac{I_{sc}}{I_{sc} - I_{opt}} \tag{22}$$

where, s_i represents the number of series connected modules. p_i represents the number of parallel connected modules. E_{STC} and T_{STC} are the irradiance and temperature values at Standard Test Conditions (STC). E and T are the given irradiance and temperature values. U_{max} and U_{min} are the maximum and minimum voltage values of the PV module. U_{opt} and I_{opt} are the optimal voltage and current values of the PV module. TCV represents the temperature coefficient value for open circuit voltage V_{oc}. TCI represents the temperature coefficient value for short circuit current I_{sc}. At standard test conditions, the parameters U'_{oc} and I'_{sc} are equal to the PV module rated parameters, U_{oc} and I_{sc}. In order to determine the validity of the proposed model, the standard parameters of the PV module are listed in Table 1.

The IV characteristics and the power curves are obtained for multiple test cases which includes the testing of the model at STC, variable irradiance levels, variable temperature levels and at both changing temperature and irradiance levels. Fig. 2 shows the performance of the model at STC. Fig. 3 shows the IV characteristics of module at different conditions.

TABLE 1. Parameters used for the validation of the proposed model.

Parameter Type	Value of Parameter
I_{sc}	4.80 A
U_{oc}	21.8 V
TCV	-0.077 V/°C
TCI	0.00206 A/°C
U_{opt}	17 V
I_{opt}	4.4 A
U_{max}	22.2 V
P_{max}	78 W

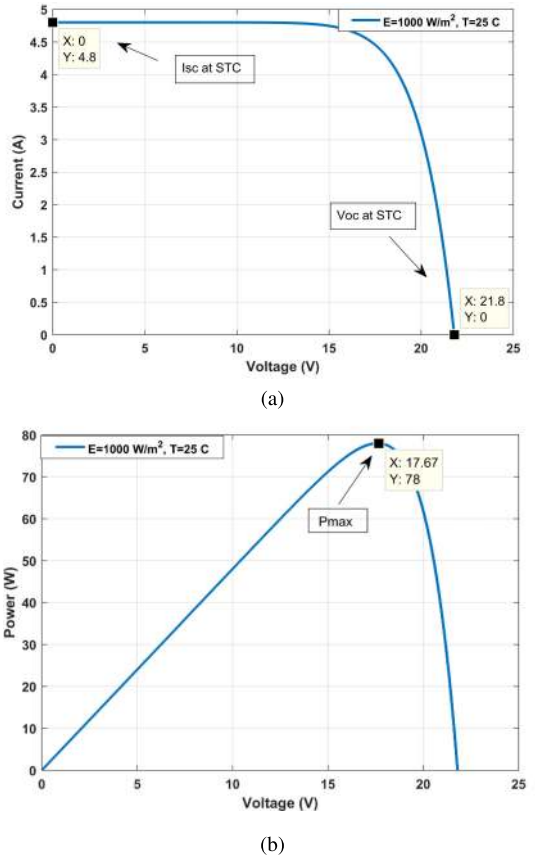

FIGURE 2. Mathematical model results at standard test conditions. (a) I-V characteristics. (b) Power curve.

It is evident from the Fig. 3 that by increasing irradiance levels, while keeping temperature constant, the short circuit current of the module increases while the open circuit voltage only changes by a small factor. On the other hand, the open circuit voltage of the module decreases at the higher temperature levels while keeping the irradiance constant. Fig. 4 shows the power curves of the module at changing atmospheric conditions.

The maximum power of the module increases as the irradiance levels are increased while keeping the temperature constant. On the other hand, the higher temperature levels decrease the maximum power output of the PV module if the irradiance is kept constant as shown in Fig. 4.

B. IRRADIANCE FORECASTING USING BOX JENKINS METHODOLOGY

The next step in the design of the PV system is to forecast the irradiance and temperature values for different scheduling

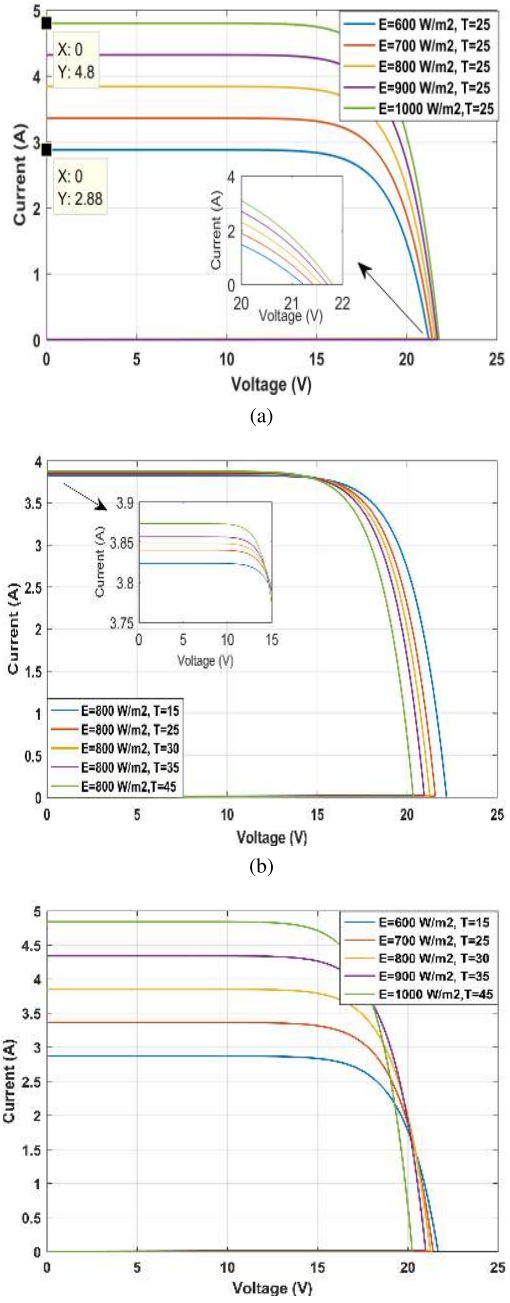

FIGURE 3. IV characteristics of the PV module at variable atmospheric conditions. (a) I-V characteristics at variable irradiance levels. (b) I-V characteristics at variable temperature levels. (c) I-V characteristics at variable temperature and irradiance levels.

intervals. A number of stochastic models and the machine learning techniques have been used by the researchers to develop the time series forecasts. One of these methods known as the Auto-Regressive Integrated Moving Average model provides reliable time series forecasts in literature [38], [39] and the same technique is adopted in this research to forecast the required parameters. This section only provides

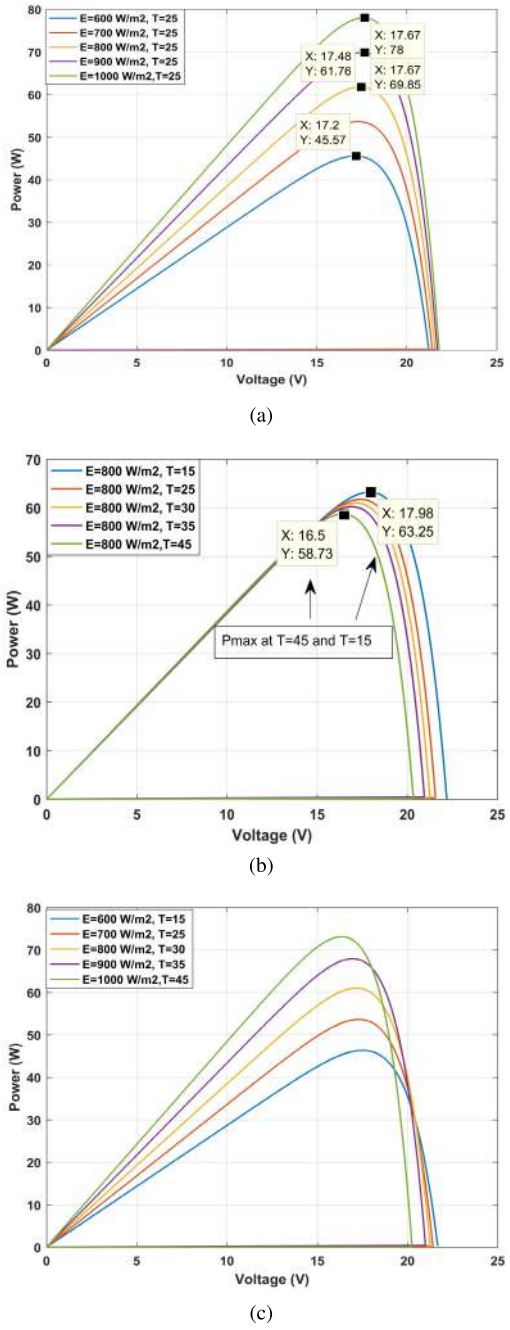

FIGURE 4. Power curves of the PV module at variable input conditions. (a) Power curve at variable irradiance levels. (b) Power curve at variable temperature levels. (c) Power curve at variable temperature and irradiance levels.

the detailed analysis required to forecast the irradiance curves for the sake of simplicity. Similar methodology can be used to forecast the temperature values.

Box-Jenkins Methodology defines the method of tuning the parameters of ARIMA(p,d,q) model for producing the time series forecasts of the desired data set [40]. The major steps involved in the Box-Jenkins Methodology are the identification of the model, the estimation of the parameters and the diagnostics of the residuals. The ARIMA model consists of the three major parts, Auto Regressive (AR) model determined by the order p, Moving Average (MA) model determined by the order q and the order of differencing d of the data set. The MA, AR and the ARMA models can be defined by the following relations.

$$X_t = \epsilon_t + \sum_{n=1}^{q} \xi_n \, \epsilon_{t-n} \tag{23}$$

$$X_t = \alpha + \sum_{n=1}^{p} \zeta_n \, X_{t-n} + \epsilon_t \tag{24}$$

$$X_t = \alpha + \epsilon_t + \sum_{n=1}^{p} \zeta_n \, X_{t-n} + \sum_{n=1}^{q} \xi_n \, \epsilon_{t-n} \tag{25}$$

where, $\zeta_1, \zeta_2 \ldots .., \zeta_n$ are the parameters of the AR model, $\xi_1, \xi_2, \ldots., \xi_n$ are the parameters of the MA model and $\epsilon_t, \epsilon_{t-1}, \epsilon_{t-2}, \ldots., \epsilon_{t-n}$ represent the white noise terms at different lags. The AR, MA and ARMA models can then be defined in the terms of the lag operator $(L^n(X_t) = X_{t-n})$ as follows:

$$\epsilon_t = (1 - \sum_{n=1}^{p} \zeta_n \, L^n) X_t = \zeta_p(L) X_t \tag{26}$$

$$X_t = (1 + \sum_{n=1}^{q} \xi_n \, L^n) \epsilon_t = \xi_q(L) \epsilon_t \tag{27}$$

$$(1 - \sum_{n=1}^{p} \zeta_n \, L^n) X_t = (1 + \sum_{n=1}^{q} \xi_n \, L^n) \epsilon_t \tag{28}$$

The additional term d in the ARIMA model is used to deal with the non-stationary data. Most of the times the data set is non-stationary in nature and requires certain measures prior to fitting the model to the data set in order to get the forecasts. The term d is used to make the data stationary and the value of d is the number of times the data set is to be differentiated before fitting the model to it. For example the first difference of the data set D_t is given by (29). By including the term d, finally the ARIMA(p,d,q) model in the terms of the lag operator is given by the (30).

$$\begin{aligned} D_t &= X_t - X_{t-1} = X_t - L^1 X_t \\ &= (1 - L^1) X_t \end{aligned} \tag{29}$$

$$(1 - \sum_{n=1}^{p} \zeta_n \, L^n)(1 - L^d) X_t = (1 + \sum_{n=1}^{q} \xi_n \, L^n) \epsilon_t \tag{30}$$

After formulating the mathematical background of the ARIMA model, the steps of the Box-Jenkins methodology are further elaborated with the help of the forecasting example. The current data set is obtained from the National Renewable Energy Laboratory (NREL) website [41] and includes the daily irradiance data for nine consecutive hours, from 8:00 AM to 5:00 PM. The data set is generated for one whole year. Fig. 5 shows the irradiance data set for the year 2015. The first step in the Box-Jenkins methodology is the identification of the model and determine the desired values

of the parameters p, d and q. The two major plots for determining these parameters are the autocorrelation plot (ACF) and partial auto correlation plot (PACF) for the given data set. The autocorrelation describes the relation between the two different lag values, for example the correlation between X_t and X_{t+n}. The partial autocorrelation describes the correlation between the two lag values by removing the effect of the intermediate lag values, for example the PACF between X_t and X_{t-6} determines the correlation between the two values without considering the effect of $X_{t-1}, X_{t-2}, \ldots.., X_{t-5}$. The range of these plots is between -1 and 1. A value of 1 indicates strong relation between the two values at different lags. A value of 0 indicates no relation. Similarly the value of -1 indicates the strong opposite relation between the two lag values. The order of p and q are determined from the PACF and ACF plots respectively. The ACF and PACF plots are obtained for the above data set and are shown in the Fig. 6.

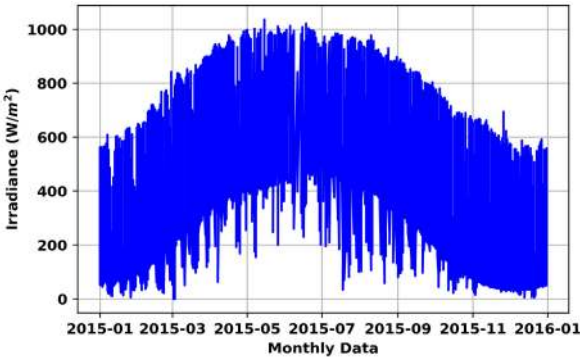

FIGURE 5. Irradiance data for the year 2015.

The plots of Fig. 6 show the significant correlation values at different lags which indicates the non-stationary behavior of the given time series. In order to make the series stationary, the first difference of the series is computed and the resulting correlation plots are shown in the Figure 7. The ACF and PACF plots fairly die down after the second lag but there are still significant values at the higher lags for the ACF plot. In order to avoid over-differentiating the time series the Augmented Dickey-Fuller (ADF) test [42] is used for checking the stationarity of the time series after taking the first difference. The ADF test includes two hypothesis, H_o and H_1. The former assumes the presence of the unit root which indicates the non stationary behavior of the given time series whereas the later indicates that no unit root is present in the data and the given time series is stationary in nature. The results for the ADF test are given in the Table 2. The p-value obtained from the ADF test is very small as compared to the critical value of 0.05, so we can easily reject the null hypothesis for a significance level of 95%, and hence the given data set is stationary after taking the first difference. The next step is to determine the value of p and q for our model. The selection of these parameters is usually difficult and it often becomes a hit and trial method. A useful method

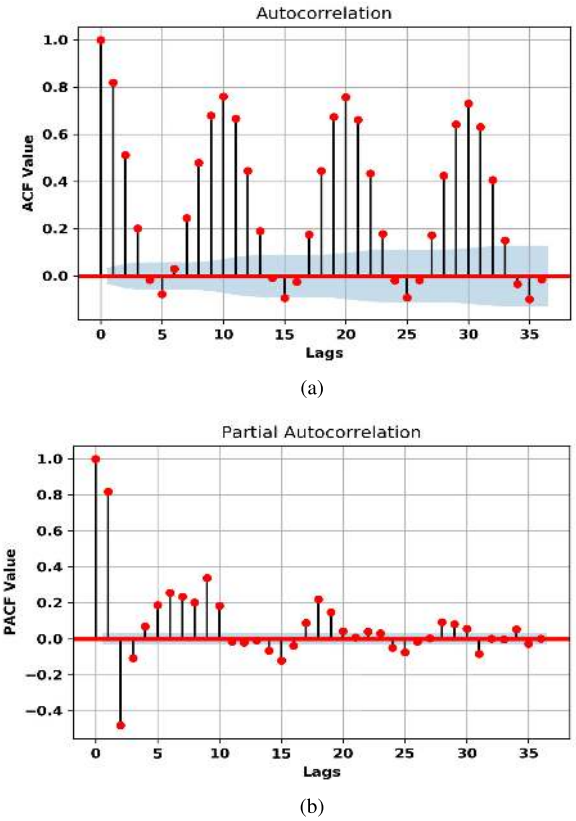

FIGURE 6. Correlation plots of the original time series. (a) ACF plot (b) PACF plot.

TABLE 2. Augmented dickey-fuller test results.

Parameter Type	Value of Parameter
ADF Statistics	-15.337
p-value	0.000
Lags	29
Observations used	3313
Critical value at 1%	-3.432
Critical value at 5%	-2.86
Critical value at 10%	-2.567

of determining these parameters is to use the information criteria values.

The two information criteria used for estimating the parameters p, d and q of the ARIMA model are the Akaike Information and Bayesian information criterion. These two criteria are the relative terms and the model having the smallest value of AIC and BIC among the group of the models is usually selected to be the best fit model. In order to determine the best model, the combination of the ARIMA models having the value of p in the range $[0, p_{max}]$, $d = 1$ and q in the range $[0, q_{max}]$ are tested and the AIC and BIC values are determined for each model. The best three models selected based on the lowest values of AIC and BIC are given in the Table 3 for p_{max} and q_{max} equal to 5. The next step is the residual diagnostics of the selected models based on the

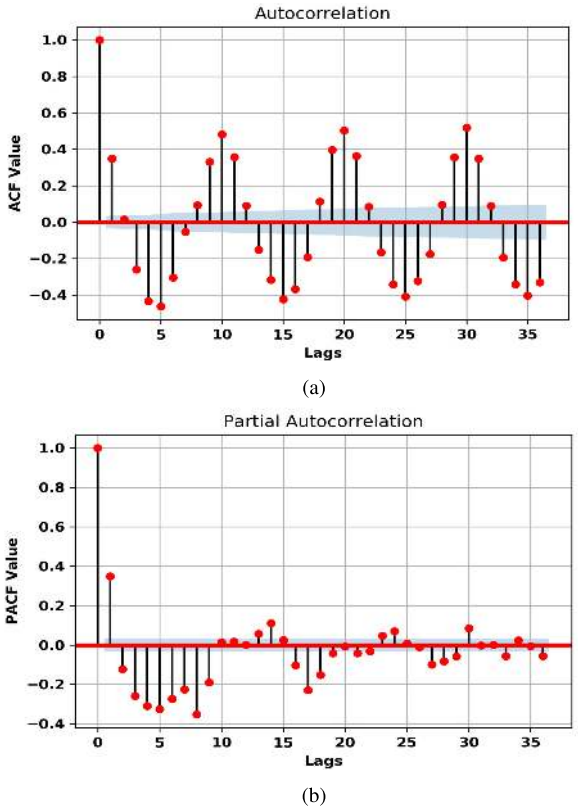

FIGURE 7. Correlation plots of the time series after taking first difference. (a) ACF plot (b) PACF plot.

values of AIC and BIC. The residual terms are primarily the error terms and they should be completely random in nature.

TABLE 3. Selection of models on the basis of AIC and BIC.

Selected Model	ARIMA(3,1,4)	ARIMA(3,1,5)	ARIMA(4,1,3)
AIC	31098	31090	31087
BIC	31151	31148	31139

There are number of methods to determine the validity of the selected model based on the residual diagnostic tests. The residual terms usually resemble the white noise having a normal distribution with zero mean and constant variance, $R \sim \mathcal{N}(0, \sigma^2)$. Moreover, the residual terms should have no correlation among them. If there exists the significant correlation among the residuals, then there will be some information missing in the selected model and a better model can be selected. The histogram, probability density function and the autocorrelation plot of the residuals for each model given in the Table 3 are determined and are shown in Fig. 8. The density and the histogram plot for each model closely resemble the normal distribution of the white noise, having the zero mean and constant variance. The ACF plot for each model shows very little correlation at certain lags, there is only a significant value at around lag seven which shows that there is still some information left which can be extracted from the model. In order to validate this assumption, the remaining models are tested, but the models selected above give the best results in the terms of the residual diagnostic tests. From the ACF plot of the three models, the model ARIMA(4,1,3) shows the smallest correlation at multiple lags except at around lag 7. However, all the models selected on the basis of information criteria are used further to produce the forecasts. The three models are trained using the 75% of the total data set, whereas the remaining data is used for the test purposes. The two error terms, the root mean squared error (RMSE) and the mean absolute error (MAE) are further used to select the final model in order to get the forecast results. The model having the smallest value of these error terms is used to get the irradiance forecast results for different scheduling intervals to compute the PV power from the mathematical model as described in the previous section. Table 4 shows the values of RMSE and MAE for the selected models.

TABLE 4. Error values for the selected models.

Model		ARIMA(3,1,4)	ARIMA(3,1,5)	ARIMA(4,1,
RMSE	$\sqrt{\frac{\sum_{i=1}^{n}(y_i'-y_i)^2}{n}}$	36.72	35.66	35.08
MAE	$\frac{\sum_{i=1}^{n}\lvert y_i'-y_i\rvert}{n}$	27.56	26.51	25.90

It is evident from Table 4 that ARIMA(4,1,3) gives the minimum value of these error terms. Therefore, the forecast results obtained from this model will be used to compute the PV power for different scheduling intervals. The forecast results are shown for the two consecutive days (30-December-2015 to 31- December-2015) for different models in Fig 9. The results obtained from ARIMA(4,1,3) will be used for computing solar power for different scheduling intervals.

C. PV POWER COMPUTATION

In order to compute the PV power using the forecasted parameters and developed mathematical model, following considerations are used:

1) The irradiance and operating temperature parameters remain constant for a particular scheduling interval i and update only at the beginning of the next interval $i+1$.
2) The power of each module for a particular scheduling interval i is determined using the irradiance and temperature values for that interval using (18)-(22). The mathematical model as described previously will be used for that purpose.
3) Each module is operating at the maximum power point.
4) The total power of the PV system is given by the sum of the individual maximum power of each module.
5) The total efficiency of the system (converter and inverter) is considered to be 95% ($\eta = 0.95$).
6) The rated system capacity is 1000 kW. The total number of PV modules required are 12821 (each module delivers the rated power of 78 W).

Under these considerations, Table 5 summarizes the results for the PV power obtained for the different scheduling inter-

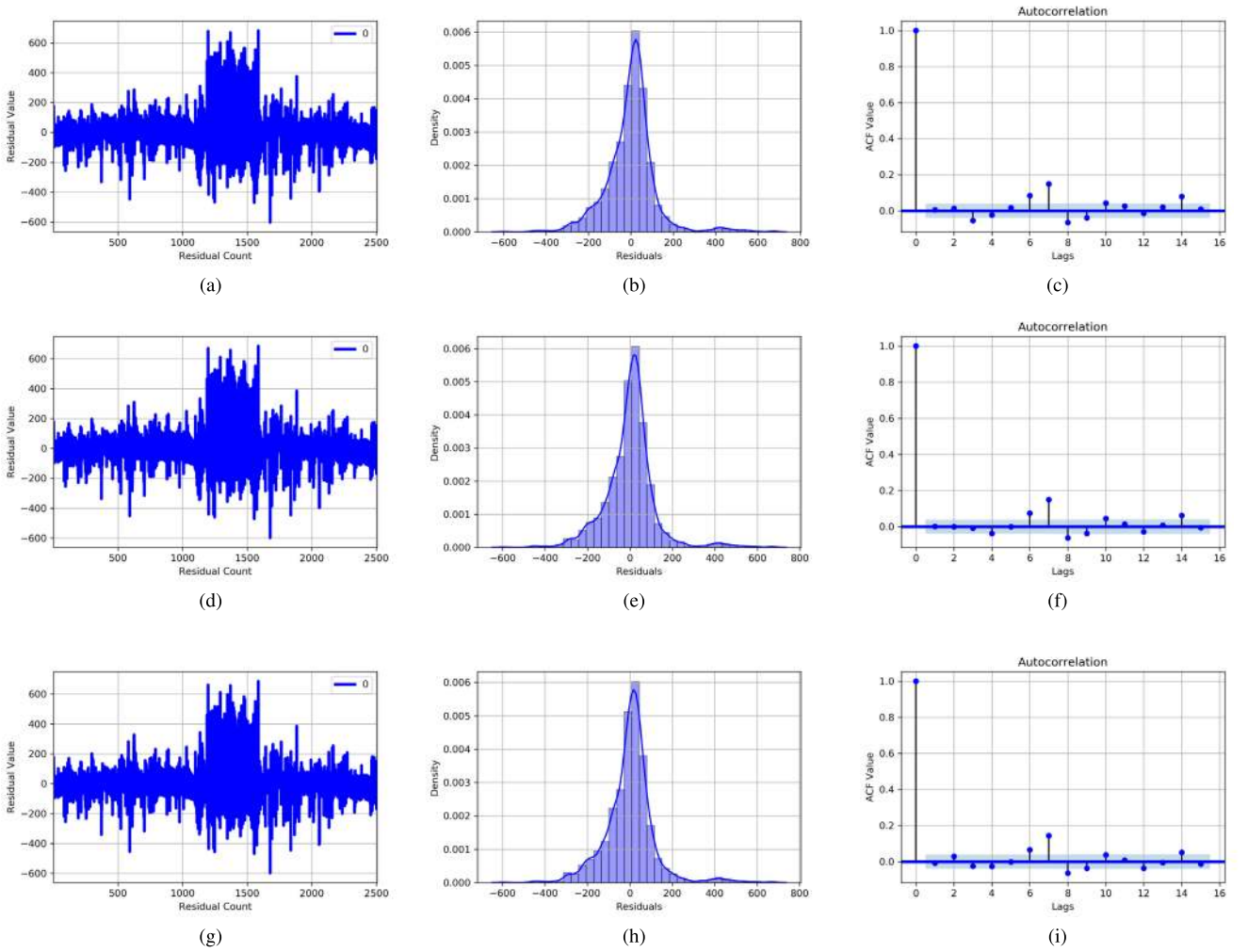

FIGURE 8. Residual diagnostic plots of different ARIMA models. (a) Residual plot of ARIMA(3,1,4). (b) Density plot of ARIMA(3,1,4). (c) ACF plot of ARIMA(3,1,4). (d) Residual plot of ARIMA(3,1,5). (e) Density plot of ARIMA(3,1,5). (f) ACF plot of ARIMA(3,1,5). (g) Residual plot of ARIMA(4,1,3). (h) Density plot of ARIMA(4,1,3), (i) ACF plot of ARIMA(4,1,3).

vals. This completes the design of the PV system for the dispatch problem. The computed solar power for different scheduling intervals will be used in determining the solar share for the main dispatch problem consisting of hydro and thermal units. The problem formulation for the suggested hybrid system consisting of both conventional and non conventional sources is elaborated in the next section.

IV. METHODOLOGY AND RESULTS

The problem of scheduling the conventional sources like hydroelectric source and thermal power source is a well known optimization problem. The fundamental concept of the STHTS problem is to minimize the fuel cost of the thermal generation while meeting the constraints of the system [43], [44]. The addition of the renewable energy resources to the conventional scheduling problem demands the up gradation of the objective function and the certain constraints related to the solar power. This section covers the detailed discussion of the short term hydrothermal scheduling problem (STHTS), the formulation of the objective function and constraints, the addition of the solar power share and the formation of the updated optimization problem. The multiple cases are explored for the suggested problem and the results of each

TABLE 5. PV power computation using mathematical model and forecasted parameters of ARIMA(4,1,3) model on 31-December-2015.

Scheduling Interval	Time (hrs)	Irradiance (W/m^2)	Operating Temperature ($^\circ$C)	P_{dc} (kW)	P_{ac} (kW)
1	8:00-9:00 AM	63.131	9	54.83	52.08
2	9:00-10:00 AM	173.90	14	157.50	149.62
3	10:00-11:00 AM	372.58	17	354.50	336.77
4	11:00-12:00 AM	494.87	19	480.00	456.00
5	12:00-13:00 PM	549.32	21	535.30	508.53
6	13:00-14:00 PM	539.00	20	525.34	499.07
7	14:00-15:00 PM	456.48	20	439.60	417.62
8	15:00-16:00 PM	343.04	18.5	324.00	307.80
9	16:00-17:00 PM	224.81	18	206.40	196.08

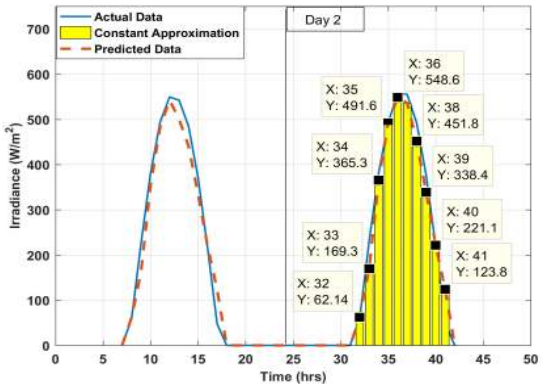

(a)

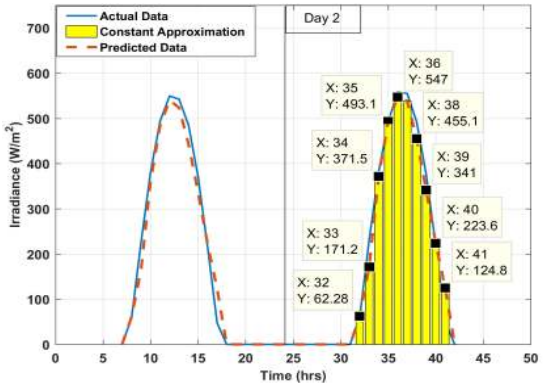

(b)

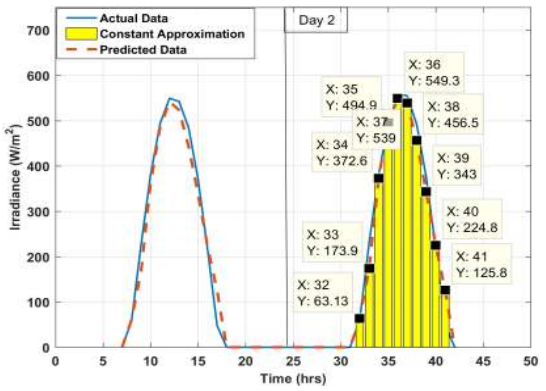

(c)

FIGURE 9. Irradiance forecast results for different models. (a) ARIMA(3,1,4). (b) ARIMA(3,1,5). (c) ARIMA (4,1,3).

case are determined using the proposed optimization methods.

A. CASE I: STHTS WITH RANDOMLY INITIALIZING THE SOLAR POWER AS PARTICLES/FIREFLIES

The Case I involves the random initialization of the solar power as particles/fireflies for each scheduling interval with in the permissible range. The objective function to be minimized includes the thermal cost as well as the solar cost of the system for each scheduling interval. Therefore, the solar cost is not fixed and is according to the initialized solar power particles. The objective function to be minimized in this case is given mathematically as follows:

$$min(f) = \sum_{i=1}^{N_s} n_i F(P_{T,i}) + C_s \sum_{i=1}^{N_s} H_i P_{S,i} \tag{31}$$

$$\text{subject to;} \quad = \begin{cases} P_{H,i} + P_{T,i} + P_{S,i} = P_{D,i} \\ P_{T,min} \leq P_{T,i} \leq P_{TH,max} \\ V_{min} \leq V_i \leq V_{max} \\ dis_{min} \leq d_i \leq dis_{max} \\ P_{H,min} \leq P_{H,i} \leq P_{H,max} \\ P_{S,min} \leq P_{S,i} \leq P_{S,max} \\ \sum_{i=1}^{N_s} n_i dis_i = dis_T \\ V_o = V_{int} \\ V_1 = V_{fin} \; \forall \; i \in \{1, 2, 3, \ldots., N_s\} \end{cases} \tag{32}$$

where, $P_{H,i}$, $P_{S,i}$, $P_{T,i}$, V_i, dis_i, $P_{D,i}$ are the values of hydro power, thermal power, solar power, volume of reservoir, discharge rate and the demand value at a particular scheduling interval i. V_o and V_1 are the starting and ending volume of the reservoir. n_i and H_i represent the duration of the scheduling interval and the duration for which the solar power remains constant for a particular scheduling interval. In our case, $n_i = H_i \; \forall \; i \in \{1, 2, 3, \ldots., N_s\}$. N_s represents the total number of scheduling intervals. The solar power limits are variable and depends upon a particular scheduling interval i. The limits for the solar power in accordance with Table 5 are defined as follows:

$$= \begin{cases} P_{S_f,i-1} \leq P_{S,i} \leq P_{S_f,i} & if \; (P_{S_f,i} \geq P_{S_f,i-1}) \\ & \wedge (P_{S_f,i} \leq P_{S_f,i+1}) \\ P_{S_f,i+1} \leq P_{S,i} \leq P_{S_f,i} & if \; (P_{S_f,i} \geq P_{S_f,i+1}) \\ & \wedge (P_{S_f,i} \leq P_{S_f,i-1}) \\ 0 \leq P_{S,i} \leq P_{S_f,i} & if \; (i = 1) \vee (i = N_s) \end{cases}$$

where, $P_{S_f,i}$ represents the forecasted solar power for a particular scheduling interval i as determined in Table 5. The volume of the reservoir and the discharge rate must be related by the equation of continuity given as follows:

$$V_i = V_{i-1} + n_i(r_i - dis_i - sp_i) \tag{33}$$

where, r_i and sp_i represent the inflow and the spillage of the water for a particular scheduling interval i.

1) STEPS OF APSO

In order, to solve the Case I, the major steps of APSO are explained as follows:

1) Find the solar forecast results and compute the maximum and minimum power limits of solar power for each scheduling interval.
2) Declare the parameters of APSO like α_1, α_2, number of particles and number of iterations. In case of Firefly

algorithm, declare constants like absorption coefficient γ_{abs} and randomization factor α.

3) Randomly initialize the volume vectors and solar power vectors as particles for all scheduling intervals within the permissible range defined by the constraints given in (32). The volume and solar power vector for a particular particle m, iteration t and N_s number of scheduling intervals are given as follows:

$$V_m^{(t)} = \begin{bmatrix} V_{1,m}^{(t)} & V_{2,m}^{(t)} & V_{3,m}^{(t)} & \cdots\cdots & V_{N_s,m}^{(t)} \end{bmatrix}^T$$
$$P_{S,m}^{(t)} = \begin{bmatrix} P_{S,1,m}^{(t)} & P_{S,2,m}^{(t)} & P_{S,3,m}^{(t)} & \cdots & P_{S,N_s,m}^{(t)} \end{bmatrix}^T$$

4) Based on the volume vectors, compute the discharge rate for each scheduling period using the equation of continuity as defined in (33) and check the limits. The discharge rate for a particular particle m, scheduling interval i and iteration t is given as follows:

$$= \begin{cases} \dfrac{(V_o - V_{1,m}^{(t)})}{n_1} & if\ i = 1 \\ \dfrac{(V_{i-1,m}^{(t)} - V_{i,m}^{(t)})}{n_i} + (r_i - sp_i) & if\ i \neq 1 \end{cases}$$

5) Compute the hydro power from the discharge rate and check the hydro power constraint given in (32). The hydro power vector for a particular particle m and iteration t is determined as the function of the discharge rate given as follows:

$$P_{H\,(N_s\times 1)}^{(t)} = \begin{bmatrix} P_{H,1,m}^{(t)} \\ P_{H,2,m}^{(t)} \\ P_{H,3,m}^{(t)} \\ . \\ . \\ . \\ P_{H,N_s,m}^{(t)} \end{bmatrix} = \begin{bmatrix} \mathbf{f}(dis_{1,m}^{(t)}) \\ \mathbf{f}(dis_{2,m}^{(t)}) \\ \mathbf{f}(dis_{3,m}^{(t)}) \\ . \\ . \\ . \\ \mathbf{f}(dis_{N_s,m}^{(t)}) \end{bmatrix}$$

6) Determine the thermal power from the power balance equation and check the thermal power constraint. The thermal vector for a particular particle m and iteration t is given as follows:

$$P_{T\,(N_s\times 1)}^{(t)} = P_{D(N_s\times 1)} - (P_{S\,(N_s\times 1)}^{(t)} + P_{H\,(N_s\times 1)}^{(t)})$$

7) Determine the total cost of the system for all scheduling intervals against all particles. The total cost for a particular particle m and iteration t is given as follows:

$$C_m^{(t)} = \alpha \sum_{j=1}^{N_s} n_j + \beta \sum_{j=1}^{N_s} n_j P_{T,j,m}^{(t)} + \gamma \sum_{j=1}^{N_s} n_j P_{T,j,m}^{2(t)} + C_s \sum_{j=1}^{N_s} H_j P_{Sj,m}^{(t)}$$

where, α, β and γ are the cost coefficients of the thermal generation.

8) Determine the particle vector corresponding to the minimum cost of the system for all scheduling intervals and declare it as the global best for the current iteration. The index of the particle corresponding to the minimum total cost is computed as follows:

$$\text{Ind} = \mathbf{min}(C_1^{(t)}, C_2^{(t)}, \ldots.., C_P^{(t)})$$

where, P are the number of particles. The global best particles for volume and solar power for a particular iteration t are given as follows:

$$V^{\prime(t)}{}_{(Ns\times 1)} = \begin{bmatrix} V_{1,\text{Ind}}^{(t)} & V_{2,\text{Ind}}^{(t)} & V_{3,\text{Ind}}^{(t)} & \cdots. & V_{N_s,\text{Ind}}^{(t)} \end{bmatrix}^T$$
$$P_S^{\prime(t)}{}_{(Ns\times 1)} = \begin{bmatrix} P_{S,1,\text{Ind}}^{(t)} & P_{S,2,\text{Ind}}^{(t)} & \cdots. & P_{S,N_s,\text{Ind}}^{(t)} \end{bmatrix}^T$$

9) Update all the solar and volume particles based on the global best using (16) and check the limits. The update equation for solar and volume vector corresponding to particular particle m and iteration t can be written as follows:

$$P_{S,m}^{(t+1)} = (1-\alpha_2)P_{S,m}^{(t)} + \alpha_2 P_S^{\prime(t)} + \alpha_1(c_1 - 0.5)$$
$$V_m^{(t+1)} = (1-\alpha_2)V_m^{(t)} + \alpha_2 V^{\prime(t)} + \alpha_1(c_1 - 0.5)$$

10) Repeat steps 4-9 until the termination criteria is achieved.

2) STEPS OF FIREFLY

The first seven steps of the firefly algorithm are same as that of the APSO. The modified steps of the firefly algorithm are given as follows:

8) Arrange the fireflies in the descending order of their total generation cost. The index array in this case can be written as follows:

$$\mathbf{Ind}_{1\times F} = \mathbf{Sort}(C_1^{(t)}, C_2^{(t)}, C_3^{(t)}, \ldots.., C_F^{(t)})$$

where, F are the number of fireflies. Rearrange the solar power and volume matrices based on the index array. Break the dimensions of the sorted solar and volume matrices across each scheduling interval. The total number of dimensions will be equal to the number of scheduling intervals N_s. The sorted solar and volume dimension against the particular scheduling interval i and iteration t are given as follows:

$$P_{S\,(1\times F)}^{(t)} = \begin{bmatrix} P_{S,i,\text{Ind}(0)}^{(t)} & P_{S,i,\text{Ind}(1)}^{(t)} & \cdots. & P_{S,i,\text{Ind}(F)}^{(t)} \end{bmatrix}$$
$$V^{(t)}{}_{(1\times F)} = \begin{bmatrix} V_{i,\text{Ind}(0)}^{(t)} & V_{i,\text{Ind}(1)}^{(t)} & V_{i,\text{Ind}(2)}^{(t)} & \cdots. & V_{i,\text{Ind}(F)}^{(t)} \end{bmatrix}$$

where, Ind(F) shows the index of the firefly corresponding to the minimum generation cost for a particular iteration t.

9) Compute the distance between the fireflies using (8). Compare all the fireflies with each other and move the firefly having lower light intensity (higher generation cost) towards the brighter firefly (lower generation cost) using (10).

10) Repeat the steps 4-9 until the termination criteria is achieved.

B. CASE II: STHTS WITH FULLY UTILIZING SOLAR POWER WHILE CONSIDERING TRANSMISSION LOSSES AND VALVE POINT EFFECT LOADING

The second case considers the solar share towards the dispatch problem to be fixed at different scheduling intervals determined from the forecasting of the parameters. The solar power at different scheduling intervals is given according to the Table 5. In this case, only the volume particles are initialized randomly whereas the solar cost is considered to be constant which is added explicitly to the converged thermal cost at the end of the scheduling problem. Therefore, the objective function in this case aims to minimize only the thermal cost of the system given as follows:

$$min(f) = \sum_{i=1}^{N_s} n_i F(P_{T,i}) \tag{34}$$

$$\text{subject to;} \quad = \begin{cases} P_{H,i} + P_{T,i} = \delta P_{D,i} + P_{L,i} \\ P_{T,min} \leq P_{T,i} \leq P_{TH,max} \\ V_{min} \leq V_i \leq V_{max} \\ dis_{min} \leq d_i \leq dis_{max} \\ P_{H,min} \leq P_{H,i} \leq P_{H,max} \\ P_{S,i} = P_{S_f,i} \\ \sum_{i=1}^{N_s} n_i dis_i = dis_T \\ V_o = V_{int} \\ V_1 = V_{fin} \quad \forall\, i \in \{1, 2, 3, \ldots, N_s\} \end{cases} \tag{35}$$

where, $\delta P_{D,i}$ and $P_{L,i}$ represent the updated demand and the losses of the system for a particular scheduling interval i. The total cost of the system in this case can be determined as follows:

$$F_{tcost} = F(P_T) + C_s \sum_{i=1}^{N_s} H_i P_{S_f,i} \tag{36}$$

where, $F(P_T)$ represents the converged cost of the system. In order to make the problem more practical, the transmission losses and the valve point effect loading is considered for the thermal power generation. The valve point effect results in the addition of an extra term in the cost equation of thermal generation, which is sinusoidal in nature. This causes the quadratic cost function to become highly non-convex and results in the formation of ripples over the smooth quadratic cost curve. The cost equation in case of valve point effect loading can be written as follows:

$$F(P_T) = \alpha + \beta P_T + \gamma P_T^2 + |dsin(f(P_{T,min} - P_T))| \tag{37}$$

1) STEPS OF APSO

In order to solve the case II, the steps of the APSO are mentioned only. The methodology of the firefly algorithm for case II is same as that of APSO except the difference of few steps which are highlighted in the previous case.

1) Find the solar power contribution for different scheduling intervals using the forecasting of the parameters as determined in Table 5.
2) Find the fixed total cost of the solar power for all scheduling intervals.
3) Find the updated demand of the system using the forecasted solar power given as follows:

$$\delta P_{D(Ns\times 1)} = P_{D(Ns\times 1)} - P_{S_{f\,(Ns\times 1)}}$$

4) Declare the parameters of APSO like α_1, α_2, number of particles and number of iterations. In case of Firefly algorithm, declare constants like absorption coefficient γ_{abs} and randomization factor α. Randomly initialize the volume vectors as particles for all scheduling intervals within the permissible range defined by the volume constraint given in (35). The volume vector for a particular particle m, iteration t and N_s number of scheduling intervals is given as follows:

$$V_m^{(t)} = \begin{bmatrix} V_{1,m}^{(t)} & V_{2,m}^{(t)} & V_{3,m}^{(t)} & \ldots\ldots & V_{N_s,m}^{(t)} \end{bmatrix}^T$$

5) Based on the volume vectors, compute the discharge rate for each scheduling period using the equation of continuity and check the limits.
6) Compute the hydro power from the discharge rate and check the hydro power constraint given in (35).
7) Determine the transmission losses of the system for all scheduling intervals. The losses are determined as the function of the hydro power computed for a particular scheduling interval i. The loss vector for a particular particle m, iteration t and N_s number of scheduling intervals is given as follows:

$$P_{L\,(Ns\times 1)}^{(t)} = \textbf{func}(P_{H\,(N_s\times 1)}^{(t)})$$

8) Determine the thermal power from the power balance equation and check the thermal power constraint. The thermal vector for a particular particle m and iteration t is given as follows:

$$P_{T\,(N_s\times 1)}^{(t)} = \delta P_{D(N_s\times 1)} + P_{L\,(Ns\times 1)}^{(t)} - P_{H\,(N_s\times 1)}^{(t)}$$

9) Determine the total cost of the system for all scheduling intervals against all particles. Determine the volume vector corresponding to the minimum cost of the system for all scheduling intervals and declare it as the global best for the current iteration.
10) Update all volume particles based on the global best using (16) and check the limits.
11) Repeat the steps 5-10 till the solution converges. Find the total cost of the system using the solar cost and the converged thermal cost of the system using (36).

The steps having the same mathematical relations as of case I are not described in the steps of APSO for case II.

C. SIMULATION PARAMETERS

The input parameters for the PV system are the forecasted irradiance and temperature levels determined in Table 5. Based on these input parameters, the forecasted solar power and the solar power limits for different scheduling intervals are listed in Table 6. For thermal and hydro units, discharge

TABLE 6. Forecasted PV power and the solar power limits for different scheduling intervals on 31-December-2015.

Scheduling Interval	Time (hrs)	P_{S_f} (MW)	Power Limits (MW)
1	8:00-9:00 AM	0.052	$0 \leq P_S \leq 0.052$
2	9:00-10:00 AM	0.149	$0.052 \leq P_S \leq 0.149$
3	10:00-11:00 AM	0.336	$0.149 \leq P_S \leq 0.336$
4	11:00-12:00 AM	0.456	$0.336 \leq P_S \leq 0.456$
5	12:00-13:00 PM	0.508	$0.456 \leq P_S \leq 0.508$
6	13:00-14:00 PM	0.499	$0.417 \leq P_S \leq 0.499$
7	14:00-15:00 PM	0.417	$0.307 \leq P_S \leq 0.417$
8	15:00-16:00 PM	0.307	$0.196 \leq P_S \leq 0.307$
9	16:00-17:00 PM	0.196	$0 \leq P_S \leq 0.196$

TABLE 7. Parameters used for validation of case I and case II.

Generation Type	Parameter	Value
Thermal Generation	$P_{T,min}$	0 MW
	$P_{T,max}$	1000 MW
Hydel Generation	$P_{H,min}$	0 MW
	$P_{H,max}$	600 MW
	V_{int}	12400 acre-ft
	V_{fin}	6000 acre-ft
	V_{min}	6000 acre-ft
	V_{max}	12000 acre-ft
	dis_{min}	0 acre-ft/hr
	dis_{max}	7000 acre-ft/hr
	r_i	3500 acre-ft/hr
	sp_i	0 acre-ft/hr
	n_i	1 hr
		$\forall\, i \in \{1, 2, .., N_s\}$
Solar Generation	C_s	0.12 \$/kWhr
	H_i	1 hr
		$\forall\, i \in \{1, 2, .., N_s\}$

rate characteristics and the thermal cost equation with and without the valve point effect loading are required. For this, a test case is developed using the data in [45], which consists of one non-pumped hydel unit having the following discharge characteristics.

$$dis(P_H) = 260 + 10P_H \quad (acre - ft/hr) \tag{38}$$

The cost characteristics of thermal generation for case I are given by (39). For case II, the thermal cost equation is given by (40).

$$F(P_T) = 575 + 9.2P_T + 0.00184P_T^2 \ \ (\$/hr) \tag{39}$$

$$P_T = 550 + 8.10P_T + 0.00028P_T^2 + |300sin(0.035(P_{T,min} - P_T))| \tag{40}$$

The transmission losses of the network (case II) for a particular scheduling interval *i* are determined as the function of the hydro power given as follows:

$$P_{L,i} = 0.00008P_{H,i}^2 \tag{41}$$

The discharge rate characteristics for case II are same as defined by (38). The remaining parameters used for the validation of the suggested dispatch problem are listed in Table 7.

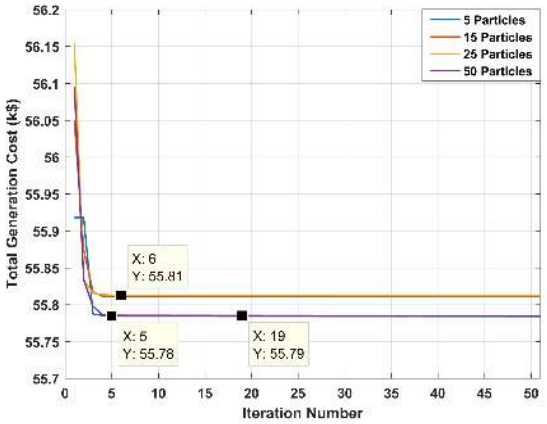

FIGURE 10. Convergence characteristics of APSO for case I using different population size.

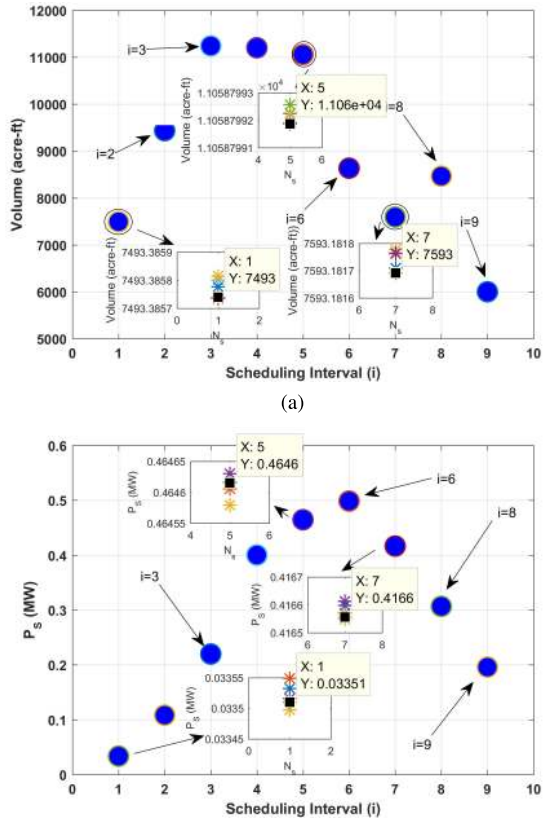

FIGURE 11. Convergence of the particles for case I using the population size of 5 particles. (a) Volume particles. (b) Solar power particles.

D. RESULTS

The results for case I and case II are determined using the parameters defined in the previous section. APSO and firefly algorithms are used to determine the convergence characteristics for both cases using the different population size.

1) RESULTS OF APSO FOR CASE I

The convergence characteristics of the case I are obtained using the APSO algorithm for different population size and are shown in the Fig. 10. The convergence graph in this

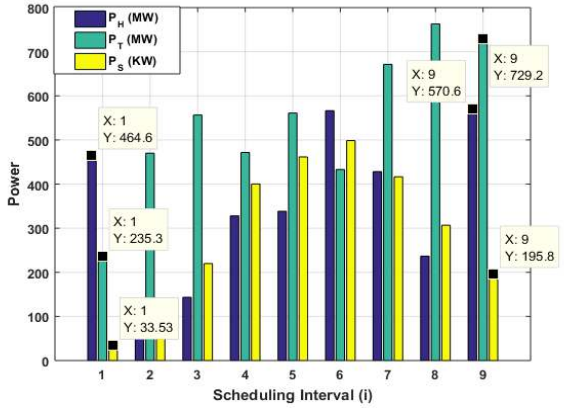

FIGURE 12. Optimal power contribution of each energy source for case I using APSO and population size of 5 particles.

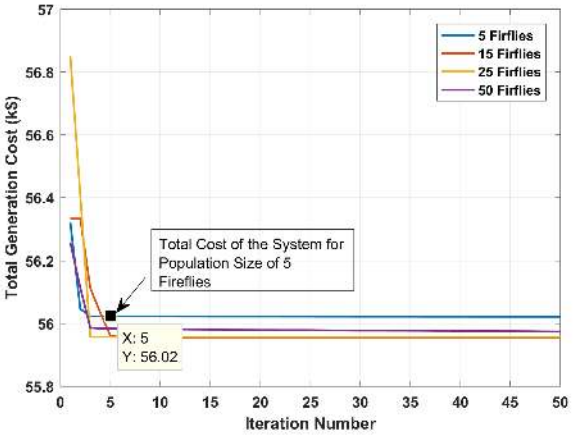

FIGURE 13. Convergence characteristics of firefly for case I using different population size.

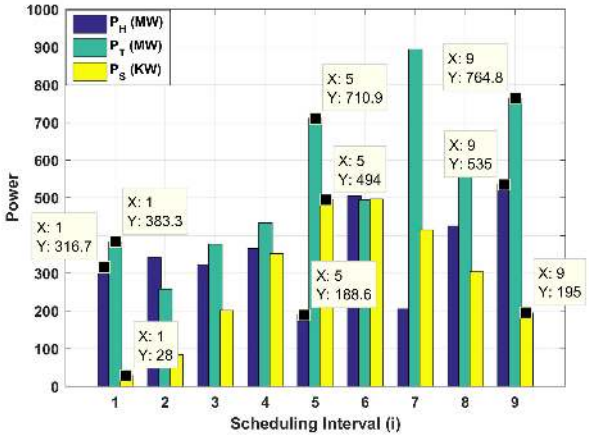

FIGURE 14. Optimal power contribution of each energy source for case I using firefly algorithm and population size of 5 fireflies.

case includes the total cost of the system for all scheduling intervals which includes both thermal and solar cost of the system. Table 8 shows the complete results of the different scheduling intervals using the APSO algorithm. The sum of

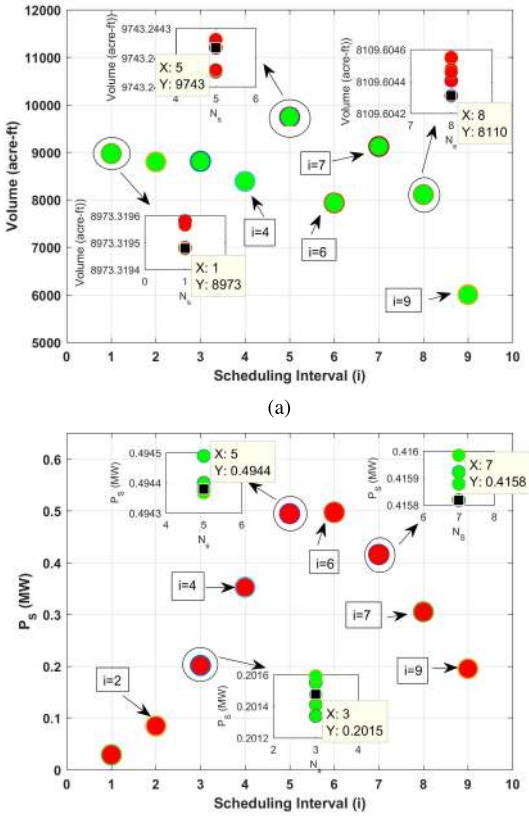

FIGURE 15. Convergence of the fireflies for case I using the population size of 5 fireflies. (a) Volume fireflies. (b) Solar power fireflies.

the power contribution from each energy source during the particular interval equals the load demand which satisfies the power balance constraint of the system. Moreover, the ending volume of the reservoir is the desired value of 6000 acre-ft which satisfies the final volume constraint of the system. The power limits are also satisfied for each scheduling interval with each energy source giving the optimal power. Fig. 11 shows the convergence of the solar and volume particles for case I. Discharge rate for any scheduling interval is computed by using the two consecutive volume values except for interval 1 which uses the starting volume of the reservoir. Fig. 12 shows the optimal power contribution of each energy source. The solar power is given in (kW) whereas, the thermal and hydo power are given in (MW).

2) RESULTS OF FIREFLY FOR CASE I

The case I is solved using the firefly algorithm for different number of fireflies and using 50 iterations for each population size. The convergence characteristics of the firefly algorithm for case I are shown in the Fig. 13. Table 9 shows the complete results of the different scheduling intervals using the firefly algorithm. For firefly algorithm, again the volume at the end of the scheduling problem is equal to 6000 acre-ft which satisfies the volume constraint. The remaining constraints like power balance constraint, the power limits and the reservoir

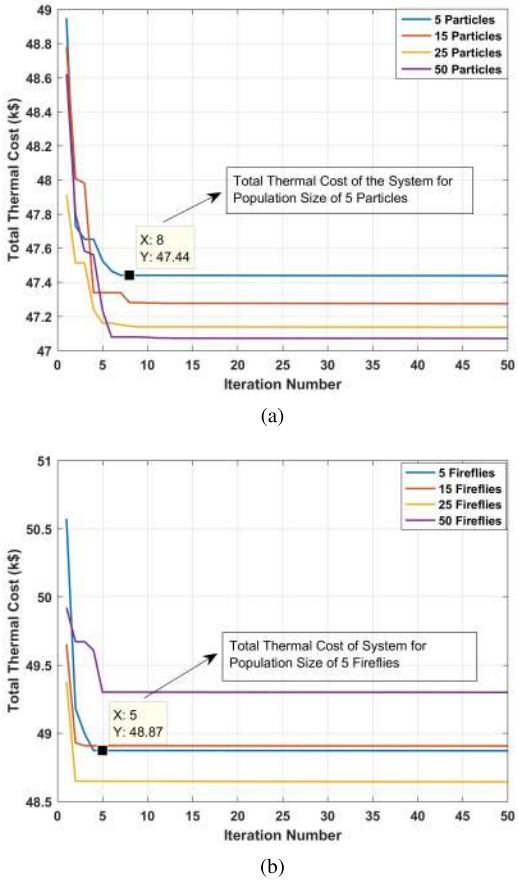

FIGURE 16. Convergence graph of case II using different number of particles/fireflies. (a) APSO algorithm. (b) Firefly algorithm.

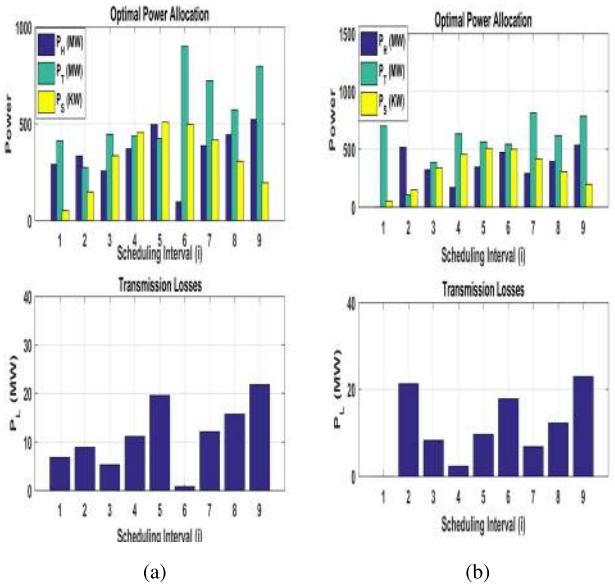

FIGURE 17. Optimal power contribution of different sources for different algorithms. (a) APSO algorithm. (b) Firefly algorithm.

constraints are also satisfied for each scheduling interval. For each scheduling interval, hydro power is computed as the

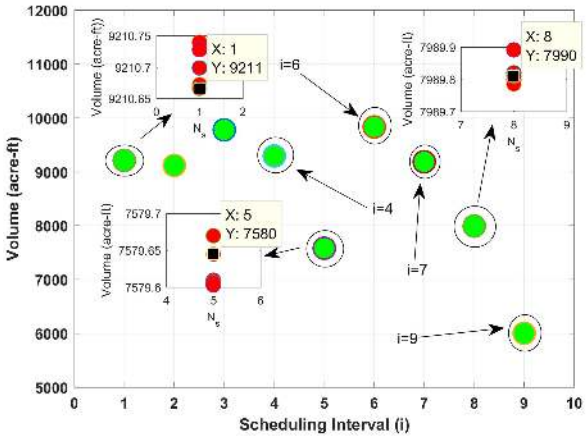

FIGURE 18. Convergence of volume particles for APSO algorithm.

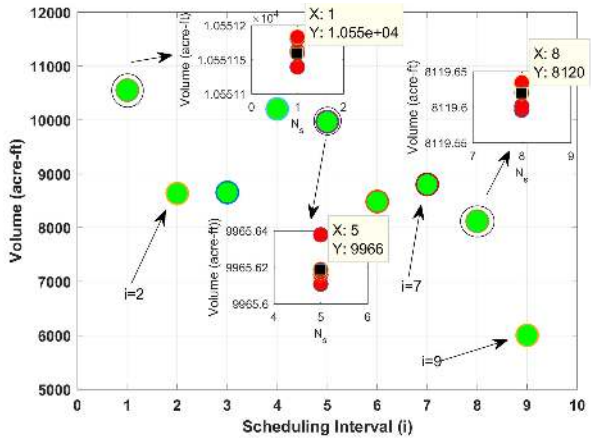

FIGURE 19. Convergence of volume particles for firefly algorithm.

function of discharge rate for that particular period using the (33). Fig. 14 shows the optimal power contribution of each energy source for case I using the firefly algorithm. Fig. 15 shows the convergence of the solar power and volume fireflies for case I using the population size of 5 fireflies.

This completes the results of the case I using both algorithms. The results of the case II which considers the transmission losses of the network and the valve point effect loading are presented in the next section

3) RESULTS OF APSO AND FIREFLY FOR CASE II

The convergence characteristics of case II are obtained using both APSO and firefly algorithm for different population size and are shown in the Fig. 16. In this case the graph only shows the total cost of the thermal generation after convergence since solar power is considered to be constant for different scheduling intervals. The optimal power contribution of different energy sources along with the transmission losses of the network are determined for each scheduling interval and are shown in the Fig. 17. The convergence of the volume particles for case II using both algorithms is shown in the Fig. 18-19. Table 10 summarizes the results of APSO and

TABLE 8. Scheduling results of case 1 using the APSO algorithm for population size of 5 particles.

Scheduling Interval	Time (hrs)	Load Demand (MW)	Optimal Power Allocation			Reservoir Parameters		Generation Cost of Energy Sources		
			P_H (MW)	P_T (MW)	P_S (MW)	Discharge Rate (acre-ft/hr)	Volume (acre-ft)	Solar Cost ($)	Thermal Cost ($)	Total Cost ($)
1	8:00-9:00	700	464.6	235.30	0.033	4906.61	7493.38	4.00	2841.68	2845.7
2	9:00-10:00	600	129.82	470.06	0.108	1558.20	9435.09	13.00	5306.14	5319.14
3	10:00-11:00	700	143.31	556.46	0.219	1693.14	11241.95	26.37	6264.24	6290.61
4	11:00-12:00	800	327.95	471.64	0.400	3539.5	11202.40	48.01	5323.43	5371.44
5	12:00-13:00	900	338.36	561.17	0.464	3643.60	11058.79	55.75	6317.26	6373.01
6	13:00-14:00	1000	566.37	433.12	0.498	5923.70	8635.07	59.83	4904.96	4964.79
7	14:00-15:00	1100	428.18	671.39	0.416	4541.80	7593.18	49.99	7581.24	7631.23
8	15:00-16:00	1000	236.73	762.96	0.306	2627.30	8465.87	36.79	8665.33	8702.12
9	16:00-17:00	1300	570.58	729.21	0.195	5965.87	6000	23.49	8262.22	8285.71
								$\sum C_S$=317.30$;	$\sum C_T$=55466$;	$\sum C_G$=55783$

TABLE 9. Scheduling results of case 1 using the firefly algorithm for population size of 5 fireflies.

Scheduling Interval	Time (hrs)	Load Demand (MW)	Optimal Power Allocation			Reservoir Parameters		Generation Cost of Energy Sources		
			P_H (MW)	P_T (MW)	P_S (MW)	Discharge Rate (acre-ft/hr)	Volume (acre-ft)	Solar Cost ($)	Thermal Cost ($)	Total Cost ($)
1	8:00-9:00	700	316.7	383.3	0.028	3426.7	8973.3	3.47	4372	4375.47
2	9:00-10:00	600	341.6	258.3	0.084	3675.9	8797.4	10.15	3074	3084.15
3	10:00-11:00	700	322.8	377.0	0.201	3487.6	8809.8	24.18	4305	4329.18
4	11:00-12:00	800	366.1	433.6	0.352	3920.8	8389.0	42.30	4910	4952.3
5	12:00-13:00	900	188.6	710.9	0.494	2145.7	9743.2	59.33	8046	8105.33
6	13:00-14:00	1000	504.7	494.8	0.497	5307.3	7935.9	59.66	5577	5636.66
7	14:00-15:00	1100	205.4	894.1	0.415	2314.4	9121.6	49.91	10272	10321.9
8	15:00-16:00	1000	425.2	574.5	0.304	4512.0	8109.6	36.57	6468	6504.57
9	16:00-17:00	1300	535.0	764.8	0.195	5609.6	6000	23.42	8688	8711.42
								$\sum C_S$=309.02$;	$\sum C_T$=55712$;	$\sum C_G$=56021$

firefly algorithm for case II using the population size of 5 particles/fireflies.

The results in Table 10 show that the total cost of the solar power remains same for both algorithms, whereas the thermal cost converges to a lower value in case of APSO for this particular sample. The sum of the power contribution from each energy source equals the demand plus the losses of the network for a particular scheduling interval. The transmission losses are directly proportional to the hydro power computed for a particular scheduling interval. The ending volume in both cases equals the desired value of 6000 acre-ft.

V. STATISTICAL COMPARISON OF APSO AND FIREFLY

The progression of the swarm based intelligence techniques such as APSO and Firefly in finding the optimal solution of the given problem depends upon the stochastic nature of the algorithm and is random in nature. Therefore, certain statistical tests are required before establishing any fact about the performance of the algorithm for a particular problem. Therefore certain statistics are used for comparing the performance of the two algorithms for each case. In literature, the comparison between the different algorithms is carried out by comparing the mean of the algorithms for a particular sample size. Although, it is an efficient method to compare the algorithms, but it can not be used to establish the fact that the significant mean difference exists for the algorithms and that the algorithms to be compared are statistically different from each other. This research uses the comparison of mean for the two algorithms to highlight which algorithm has a lower mean generation cost and then uses the independent t test results to show that the significant mean difference exists between the algorithms and the two techniques are statistically different from each other. Table 11 shows the comparison of the performance parameters of APSO and firefly algorithm for case I. Table 12 shows the comparison of algorithms for case II. Table 13 shows the results of independent t-test results for both cases. From the Table 11 and Table 12, it is evident that APSO gives lower mean generation

TABLE 10. Scheduling results of case II for APSO and firefly algorithm.

Scheduling Results for APSO

Scheduling Interval	Load Demand (MW)	P_L (MW)	Optimal Power Allocation			Reservoir Parameters		Generation Cost of Energy Sources		
			P_H (MW)	P_T (MW)	P_S (MW)	Discharge Rate (acre-ft/hr)	Volume (acre-ft)	Solar Cost ($)	Thermal Cost ($)	Total Cost ($)
1	700	6.86	292.29	413.88	0.052	3189	9210	6.23	4232	4238.23
2	600	8.88	333.27	275.45	0.149	3592	9117	17.87	2866	2883.8
3	700	5.32	258.03	446.95	0.336	2840	9777	40.32	4245	4285.3
4	800	11.10	372.51	438.13	0.456	3985	9292	54.71	4262	4316.7
5	900	19.62	495.28	423.83	0.508	5212	7579	60.96	4263	4323.9
6	1000	0.77	98.70	901.56	0.499	1247	9832	59.88	8121	8180.8
7	1100	12.08	388.64	723.01	0.417	4146	9186	50.03	6604	6654.03
8	1000	15.74	443.62	571.81	0.307	4696	7989	36.83	5548	5584.83
9	1300	21.88	522.98	798.70	0.196	5489	6000	23.52	7292	7315.52
								$\sum C_S$=350.3$;	$\sum C_T$=47437$;	$\sum C_G$=47788$

Scheduling Results for Firefly

Scheduling Interval	Load Demand (MW)	P_L (MW)	Optimal Power Allocation			Reservoir Parameters		Generation Cost of Energy Sources		
			P_H (MW)	P_T (MW)	P_S (MW)	Discharge Rate (acre-ft/hr)	Volume (acre-ft)	Solar Cost ($)	Thermal Cost ($)	Total Cost ($)
1	700	0	0	699.94	0.052	0	10551	6.23	6534	6540.23
2	600	21.3	515.9	105.3	0.149	5418	8633	17.87	1560	1577.87
3	700	8.3	322.1	385.8	0.336	3481	8651	40.32	3959	3999.32
4	800	2.3	168.8	633.0	0.456	1948	10203	54.71	5838	5892.71
5	900	9.7	347.8	561.4	0.508	3737	9966	60.96	5400	5460.96
6	1000	17.8	472.2	545.1	0.499	4982	8483	59.88	5117	5176.88
7	1100	6.8	292.2	814.2	0.417	3182	8801	50.03	7396	7446.03
8	1000	12.3	392.1	619.9	0.307	4181	8120	36.83	5766	5802.83
9	1300	23.0	536.0	786.8	0.196	5619	6000	23.52	7297	7320.52
								$\sum C_S$=350.3$;	$\sum C_T$=48871$;	$\sum C_G$=49221$

TABLE 11. Statistical evaluation of two algorithms for case I using different population size, 50 iterations and 50 samples of each algorithm.

Performance Parameter	Firefly Algorithm	APSO Algorithm
Evaluation of parameters for population size of 5 particles/fireflies		
Average Cost	56260 $	55548 $
Minimum Cost	55278 $	54972 $
Maximum Cost	57108 $	56471 $
Average Computation Time	0.5951 s	0.80 s
Maximum Computation Time	0.815 s	1.00 s
Minimum Computation Time	0.45 s	0.7 s
Number of Convergences	87 out of 100	84 out of 100
Average computation time for different fireflies/particles		
Average Computation Time (15 Fireflies/Particles)	0.78 s	0.94 s
Average Computation Time (25 Fireflies/Particles)	0.81 s	0.99 s
Average Computation Time (50 Fireflies/Particles)	0.82 s	1.00 s

TABLE 12. Statistical evaluation of two algorithms for case II using different population size, 50 iterations and 50 samples of each algorithm.

Performance Parameter	Firefly Algorithm	APSO Algorithm
Evaluation of parameters for population size of 5 particles/fireflies		
Average Cost	49049 $	47116 $
Minimum Cost	47603 $	46203 $
Maximum Cost	51601 $	47991 $
Average Computation Time	0.497 s	0.519 s
Maximum Computation Time	0.571 s	0.556 s
Minimum Computation Time	0.443 s	0.499 s
Number of Convergences	85 out of 100	83 out of 100
Average computation time for different fireflies/particles		
Average Computation Time (15 Fireflies/Particles)	0.515 s	0.637 s
Average Computation Time (25 Fireflies/Particles)	0.571 s	0.658 s
Average Computation Time (50 Fireflies/Particles)	0.620 s	0.703 s

cost whereas the execution time of the firefly algorithm is better than the APSO technique. To analyze the independent t-test results, the significant values for Levene's test and the t-test for equality of means are considered. If the significant value for Levene's test is greater than the critical value of 0.05, we can say that the two algorithms have statistically same variance for a confidence level of 95%. On the other hand, if the significant value for the t-test for equality of means is less than the critical value of 0.05, we can say that the two algorithms are statistically different from each other and

TABLE 13. Independent t-test for comparison of means of two algorithms using the population size of 5 particles/fireflies, 50 iterations and 50 samples of each algorithm.

Independent t-test results for case I									
	Levene's Test for Equality of Variances		t-test for Equality of Means					95% Confidence level of Difference	
	F	Sig.	t	df	Sig. (2-tailed)	Mean Difference	Std. Error Difference	Lower	Upper
Equal variances assumption	1.57	.21	-5.09	98	.000	-711.1	139.4	-987.8	-434.3
Unequal variances			-5.09	92.3	.000	-711.1	139.4	-988.05	-434.1
Independent t-test results for case II									
	Levene's Test for Equality of Variances		**t-test for Equality of Means**					**95% Confidence level of Difference**	
	F	**Sig.**	**t**	**df**	**Sig. (2-tailed)**	**Mean Difference**	**Std. Error Difference**	**Lower**	**Upper**
Equal variances assumption	3.486	.065	-16.42	98	.000	-1932	117.65	-2165.95	-1698.98
Equal variances not assumed			-16.425	79.92	.000	-1932	117.65	-2166.61	-1698.32

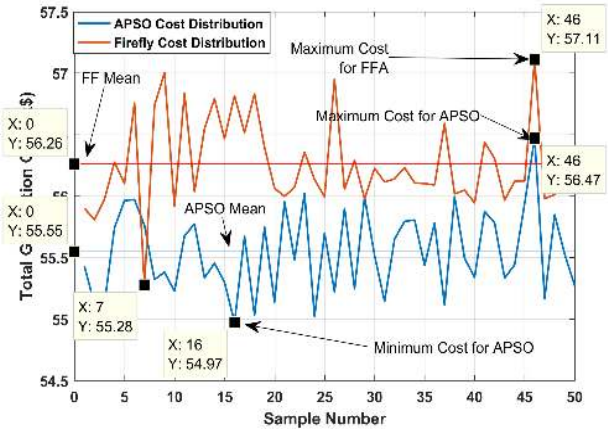

FIGURE 20. Cost distribution of algorithms for case I.

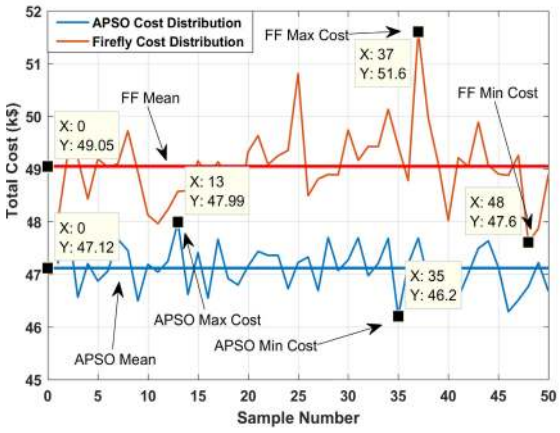

FIGURE 21. Cost distribution of algorithms for case II.

have significant statistical mean difference. From Table 13, it is evident that for both cases, APSO and firefly algorithm have same variance statistically, whereas there exists the significant mean difference between the two techniques and the suggested algorithms are statistically different from each other for both cases based on the mean generation cost. Fig. 20-21 show the cost distribution for both cases using the APSO and the firefly algorithm.

VI. CONCLUSION

The proposed research presents a novel STHTS problem with the addition of the photovoltaic energy source and presents a modified methodology to solve the dispatch problem while considering the intermittent nature of the PV source. The forecasting of the PV input parameters and the mathematical modeling of the PV module give accurate results regarding the solar share towards the dispatch problem thus incorporating the effect of the atmospheric conditions on the output power of the PV source. The two meta-heuristic techniques namely APSO and firefly algorithms are explored for the various test cases while considering the multiple system constraints. The suggested algorithms successfully solve the dispatch problem without violating the system constraints and reduce the overall generation cost of the system by intelligently utilizing the different energy resources during

different scheduling intervals. Moreover, due to the stochastic nature of the meta-heuristic techniques, different statistical methods are suggested to efficiently compare the performance of the two algorithms. The APSO technique outperforms the firefly algorithm and gives a overall lower mean generation cost. Although, the firefly algorithm gives relatively higher mean generation cost, the execution time of the respective algorithm is better than its corresponding algorithm. The future research involves the optimal tuning of the input parameters of the algorithms in order to further reduce the generation cost of the system. Moreover, wind energy systems and different renewable energy sources can be added to the suggested hybrid energy system to further explore the effect of adding the distributed generation systems to the conventional grid.

REFERENCES

[1] T. G. Hlalele, R. M. Naidoo, J. Zhang, and R. C. Bansal, "Dynamic economic dispatch with maximal renewable penetration under renewable obligation," *IEEE Access*, vol. 8, pp. 38794–38808, 2020.
[2] W. Yi, Y. Zhang, Z. Zhao, and Y. Huang, "Multiobjective robust scheduling for smart distribution grids: Considering renewable energy and demand response uncertainty," *IEEE Access*, vol. 6, pp. 45715–45724, 2018.
[3] K. Tian, W. Sun, D. Han, and C. Yang, "Coordinated planning with predetermined renewable energy generation targets using extended two-stage robust optimization," *IEEE Access*, vol. 8, pp. 2395–2407, 2020.
[4] S. Fan, Z. Li, Z. Li, and G. He, "Evaluating and increasing the renewable energy share of customer's electricity consumption," *IEEE Access*, vol. 7, pp. 129200–129214, 2019.
[5] M. B. Rasheed, M. A. Qureshi, N. Javaid, and T. Alquthami, "Dynamic pricing mechanism with the integration of renewable energy source in smart grid," *IEEE Access*, vol. 8, pp. 16876–16892, 2020.
[6] J. Yu, C. Dou, and X. Li, "MAS-based energy management strategies for a hybrid energy generation system," *IEEE Trans. Ind. Electron.*, vol. 63, no. 6, pp. 3756–3764, Jun. 2016.
[7] A. A. Hadi, C. A. S. Silva, E. Hossain, and R. Challoo, "Algorithm for demand response to maximize the penetration of renewable energy," *IEEE Access*, vol. 8, pp. 55279–55288, 2020.
[8] Y. Jia, Z. Y. Dong, C. Sun, and K. Meng, "Cooperation-based distributed economic MPC for economic load dispatch and load frequency control of interconnected power systems," *IEEE Trans. Power Syst.*, vol. 34, no. 5, pp. 3964–3966, Sep. 2019.
[9] E. Gil, J. Bustos, and H. Rudnick, "Short-term hydrothermal generation scheduling model using a genetic algorithm," *IEEE Trans. Power Syst.*, vol. 18, no. 4, pp. 1256–1264, Nov. 2003.
[10] M. Basu, "An interactive fuzzy satisfying method based on evolutionary programming technique for multiobjective short-term hydrothermal scheduling," *Electr. Power Syst. Res.*, vol. 69, nos. 2–3, pp. 277–285, May 2004.
[11] K. K. Mandal, M. Basu, and N. Chakraborty, "Particle swarm optimization technique based short-term hydrothermal scheduling," *Appl. Soft Comput.*, vol. 8, no. 4, pp. 1392–1399, Sep. 2008.
[12] P. K. Roy, "Teaching learning based optimization for short-term hydrothermal scheduling problem considering valve point effect and prohibited discharge constraint," *Int. J. Electr. Power Energy Syst.*, vol. 53, pp. 10–19, Dec. 2013.
[13] N. Sinha, R. Chakrabarti, and P. K. Chattopadhyay, "Fast evolutionary programming techniques for short-term hydrothermal scheduling," *IEEE Trans. Power Syst.*, vol. 18, no. 1, pp. 214–220, Feb. 2003.
[14] T. T. Nguyen, D. N. Vo, and A. V. Truong, "Cuckoo search algorithm for short-term hydrothermal scheduling," *Appl. Energy*, vol. 132, no. 1, pp. 276–287, Nov. 2014.
[15] S. Ghosh, M. Kaur, S. Bhullar, and V. Karar, "Hybrid abc-bat for solving short-term hydrothermal scheduling problems," *Energies*, vol. 12, no. 3, pp. 551–566, 2019.
[16] M. Nazari-Heris, A. F. Babaei, B. Mohammadi-Ivatloo, and S. Asadi, "Improved harmony search algorithm for the solution of non-linear non-convex short-term hydrothermal scheduling," *Energy*, vol. 151, pp. 226–237, May 2018.
[17] P. K. Roy, M. Pradhan, and T. Paul, "Krill herd algorithm applied to short-term hydrothermal scheduling problem," *Ain Shams Eng. J.*, vol. 9, no. 1, pp. 31–43, Mar. 2018.
[18] M. S. Fakhar, S. A. R. Kashif, M. A. Saqib, and T. U. Hassan, "Non cascaded short-term hydro-thermal scheduling using fully-informed particle swarm optimization," *Int. J. Electr. Power Energy Syst.*, vol. 73, pp. 983–990, Dec. 2015.
[19] N. A. Khan, G. A. S. Sidhu, and F. Gao, "Optimizing combined emission economic dispatch for solar integrated power systems," *IEEE Access*, vol. 4, pp. 3340–3348, 2016.
[20] Q. Zhang, X. Wang, T. Yang, and J. Liang, "Research on scheduling optimisation for an integrated system of wind-photovoltaic-hydro-pumped storage," *J. Eng.*, vol. 2017, no. 13, pp. 1210–1214, Jan. 2017.
[21] C. Peng, P. Xie, L. Pan, and R. Yu, "Flexible robust optimization dispatch for hybrid Wind/Photovoltaic/Hydro/Thermal power system," *IEEE Trans. Smart Grid*, vol. 7, no. 2, pp. 751–762, Mar. 2016.
[22] N. Saxena and S. Ganguli, "Solar and wind power estimation and economic load dispatch using firefly algorithm," *Procedia Comput. Sci.*, vol. 70, pp. 688–700, Jan. 2015.
[23] S. A. Alavi, A. Ahmadian, and M. Aliakbar-Golkar, "Optimal probabilistic energy management in a typical micro-grid based-on robust optimization and point estimate method," *Energy Convers. Manage.*, vol. 95, pp. 314–325, May 2015.
[24] R. O. Eni and J.-F.-K. Akinbami, "Flexibility evaluation of integrating solar power into the nigerian electricity grid," *IET Renew. Power Gener.*, vol. 11, no. 2, pp. 239–247, Feb. 2017.
[25] V. K. Jadoun, V. C. Pandey, N. Gupta, K. R. Niazi, and A. Swarnkar, "Integration of renewable energy sources in dynamic economic load dispatch problem using an improved fireworks algorithm," *IET Renew. Power Gener.*, vol. 12, no. 9, pp. 239–247, 2018.
[26] M. Basu, "Combined heat and power dynamic economic dispatch with demand side management incorporating renewable energy sources and pumped hydro energy storage," *IET Gener., Transmiss. Distrib.*, vol. 13, no. 17, pp. 3771–3781, Sep. 2019.
[27] M. K. Marichelvam, T. Prabaharan, and X. S. Yang, "A discrete firefly algorithm for the multi-objective hybrid flowshop scheduling problems," *IEEE Trans. Evol. Comput.*, vol. 18, no. 2, pp. 301–305, Apr. 2014.
[28] B. Khan and P. Singh, "Selecting a meta-heuristic technique for smart micro-grid optimization problem: A comprehensive analysis," *IEEE Access*, vol. 5, pp. 13951–13977, 2017.
[29] S. L. Ho, S. Yang, G. Ni, E. W. C. Lo, and H. C. Wong, "A particle swarm optimization-based method for multiobjective design optimizations," *IEEE Trans. Magn.*, vol. 41, no. 5, pp. 1756–1759, May 2005.
[30] Y. Yang, B. Wei, H. Liu, Y. Zhang, J. Zhao, and E. Manla, "Chaos firefly algorithm with self-adaptation mutation mechanism for solving large-scale economic dispatch with valve-point effects and multiple fuel options," *IEEE Access*, vol. 6, pp. 45907–45922, 2018.
[31] T. Niknam, R. Azizipanah-Abarghooee, and A. Roosta, "Reserve constrained dynamic economic dispatch: A new fast self-adaptive modified firefly algorithm," *IEEE Syst. J.*, vol. 6, no. 4, pp. 635–646, Dec. 2012.
[32] M. Zhang, Z. Chen, and L. Wei, "An immune firefly algorithm for tracking the maximum power point of PV array under partial shading conditions," *Energies*, vol. 12, no. 16, p. 3083, Aug. 2019.
[33] X. S. Yang, "Firefly algorithm," in *Engineering Optimization: An Introduction with Metaheuristic Applications*, 2nd ed. Hoboken, NJ, USA: Wiley, 2010, ch. 17, sec. 2, pp. 221–229.
[34] P. K. Hota, A. K. Barisal, and R. Chakrabarti, "An improved PSO technique for short-term optimal hydrothermal scheduling," *Electr. Power Syst. Res.*, vol. 79, no. 7, pp. 1047–1053, Jul. 2009.
[35] Y. Mahmoud and E. El-Saadany, "Accuracy improvement of the ideal PV model," *IEEE Trans. Sustain. Energy*, vol. 6, no. 3, pp. 909–911, Jul. 2015.
[36] Y. Mahmoud, W. Xiao, and H. H. Zeineldin, "A simple approach to modeling and simulation of photovoltaic modules," *IEEE Trans. Sustain. Energy*, vol. 3, no. 1, pp. 185–186, Jan. 2012.
[37] E. I. Ortiz-Rivera, "Approximation of a photovoltaic module model using fractional and integral polynomials," in *Proc. IEEE PVSC*, Austin, TX, USA, Jun. 2012, pp. 2927–2931.
[38] M. Khashei, M. Bijari, and S. R. Hejazi, "Combining seasonal ARIMA models with computational intelligence techniques for time series forecasting," *Soft Comput.*, vol. 16, no. 6, pp. 1091–1105, Jun. 2012.
[39] K. Yunus, T. Thiringer, and P. Chen, "ARIMA-based frequency-decomposed modeling of wind speed time series," *IEEE Trans. Power Syst.*, vol. 31, no. 4, pp. 2546–2556, Jul. 2016.

[40] P. Paretkar, L. Mili, V. Centeno, K. Jin, and C. Miller, "Short-term forecasting of power flows over major transmission interties: Using Box and Jenkins ARIMA methodology," in *Proc. IEEE PES-GM*, Providence, RI, USA, Jul. 2010, pp. 25–29.
[41] A. Andreas and S. Wilcox, "Solar resource and meteorological assessment project (SOLRMAP)," Rotating Shadowband Radiometer, Los Angeles, CA, USA, Tech. Rep. DA-5500-56502, 2012, doi: 10.5439/1052230.
[42] B. Li, J. Zhang, Y. He, and Y. Wang, "Short-term load-forecasting method based on wavelet decomposition with second-order gray neural network model combined with ADF test," *IEEE Access*, vol. 5, pp. 16324–16331, 2017.
[43] J. J. Chen and J. H. Zheng, "Discussion on 'short-term environmental/economic hydrothermal scheduling,'" *Electr. Power Syst. Res.*, vol. 127, pp. 348–350, Oct. 2015.
[44] H. Zhang, J. Zhou, Y. Zhang, N. Fang, and R. Zhang, "Short term hydrothermal scheduling using multi-objective differential evolution with three chaotic sequences," *Int. J. Electr. Power Energy Syst.*, vol. 47, pp. 85–99, May 2013.
[45] M. S. Fakhar, S. A. R. Kashif, N. U. Ain, H. Z. Hussain, A. Rasool, and I. A. Sajjad, "Statistical performances evaluation of APSO and improved APSO for short term hydrothermal scheduling problem," *Appl. Sci.*, vol. 9, no. 12, p. 2440, Jun. 2019.

SHEROZE LIAQUAT received the bachelor's degree in electrical engineering with a specialization in power systems from the University of Engineering and Technology, Lahore, Pakistan, where he is currently pursuing the master's degree with a specialization in the power systems analysis. He is also serving as a Lab Instructor with the Department of Electrical Engineering, National University of Computer and Emerging Sciences, Lahore. His current research interests include the applications of meta-heuristic techniques in distributed generation systems, and the optimal scheduling of conventional and non-conventional sources.

MUHAMMAD SALMAN FAKHAR received the bachelor's and master's degrees in electrical engineering with a specialization in power systems from the University of Engineering and Technology (UET), Lahore, Pakistan, where he is currently pursuing the Ph.D. degree with a specialization in the design of novel meta-heuristic algorithms for variants of short term hydrothermal scheduling problem. He is currently serving as a Lecturer with the Department of Electrical Engineering, UET. His current research interests include the applications of meta-heuristic techniques and their variants for optimal scheduling of conventional sources, and the investigation of short-term hydrothermal scheduling problems.

SYED ABDUL RAHMAN KASHIF received the B.Sc., M.Sc., and Ph.D. degrees in electrical engineering from the University of Engineering and Technology (UET), Lahore, Pakistan. He worked as a Researcher with the Power Electronics Laboratory, University of Paderborn, Germany, from 2009 to 2010. He is currently serving as an Associate Professor with the Department of Electrical Engineering, UET. His research interests include power electronics, the control of electrical machines, smart grids, renewable energy systems, and the optimization of power systems.

AKHTAR RASOOL received the Ph.D. degree in mechatronics engineering from Sabanci University, Turkey. He is currently serving as an Assistant Professor and the Director of Quality Cell with the Sharif College of Engineering and Technology, Lahore, Pakistan. His major research interest includes the control of converters with applications ranging the integration of renewable energy resources, microgrids, smartgrids, electrical machines, automated electrical vehicles, electrical trains, automatic braking, steering, robotic actuators, energy management, process control, cascaded control applications, and high voltage engineering.

OMER SALEEM (Member, IEEE) received the bachelor's and master's degrees in electrical engineering with a specialization in control systems from the University of Engineering and Technology (UET), Lahore, Pakistan, where he is currently pursuing the Ph.D. degree with a specialization in adaptive control systems. He is also serving as an Assistant Professor with the Department of Electrical Engineering, National University of Computer and Emerging Sciences, Lahore. His research interests include the design of adaptive and self-tuning control systems for mechatronic systems and power electronic converters.

SANJEEVIKUMAR PADMANABAN (Senior Member, IEEE) received the bachelor's degree in electrical engineering from the University of Madras, Chennai, India, in 2002, the master's degree (Hons.) in electrical engineering from Pondicherry University, Puducherry, India, in 2006, and the Ph.D. degree in electrical engineering from the University of Bologna, Italy, in 2012. He was an Associate Professor with the VIT University from 2012 to 2013. In 2013, he joined the National Institute of Technology, India, as a Faculty Member. In 2014, he was invited as a Visiting Researcher with the Department of Electrical Engineering, Qatar University, Doha, Qatar, funded by the Qatar National Research Foundation (Government of Qatar). He continued his research activities with the Dublin Institute of Technology, Dublin, Ireland, in 2014. He was an Associate Professor with the Department of Electrical and Electronics Engineering, University of Johannesburg, Johannesburg, South Africa, from 2016 to 2018. Since 2018, he has been a Faculty Member of the Department of Energy Technology, Aalborg University, Esbjerg, Denmark. He has authored more than 300 scientific articles. He is a Fellow of the Institution of Engineers, India, the Institution of Electronics and Telecommunication Engineers, India, and the Institution of Engineering and Technology, U.K. He was a recipient of the Best Paper cum Most Excellence Research Paper Award from IET-SEISCON in 2013, IET-CEAT in 2016, the IEEE-EECSI in 2019, and the IEEE-CENCON in 2019, and five best paper awards from ETAEERE in 2016, sponsored Lecture Notes in Electrical Engineering, a Springer book.